

RESEARCH

Open Access



# Active full-length DNA A $\beta$ <sub>42</sub> immunization in 3xTg-AD mice reduces not only amyloid deposition but also tau pathology

Roger N. Rosenberg, Min Fu and Doris Lambracht-Washington\* 

## Abstract

**Background:** Alzheimer's disease (AD) is the most well-known and most common type of age-related dementia. Amyloid deposition and hyperphosphorylation of tau protein are both pathological hallmarks of AD. Using a triple-transgenic mouse model (3xTg-AD) that develops plaques and tangles in the brain similar to human AD, we provide evidence that active full-length DNA amyloid- $\beta$  peptide 1–42 (A $\beta$ <sub>42</sub>) trimer immunization leads to reduction of both amyloid and tau aggregation and accumulation.

**Methods:** Immune responses were monitored by enzyme-linked immunosorbent assay (ELISA) (antibody production) and enzyme-linked immunospot (cellular activation, cytokine production). Brains from 20-month-old 3x Tg-AD mice that had received DNA A $\beta$ <sub>42</sub> immunotherapy were compared with brains from age- and gender-matched transgenic A $\beta$ <sub>42</sub> peptide-immunized and control mice by histology, Western blot analysis, and ELISA. Protein kinase activation and kinase levels were studied in Western blots from mouse hemibrain lysates.

**Results:** Quantitative ELISA showed a 40% reduction of A $\beta$ <sub>42</sub> peptide and a 25–50% reduction of total tau and different phosphorylated tau molecules in the DNA A $\beta$ <sub>42</sub> trimer-immunized 3xTg-AD mice compared with nonimmunized 3xTg-AD control animals. Plaque and A $\beta$  peptide reductions in the brain were due to the anti-A $\beta$  antibodies generated following the immunizations. Reductions of tau were likely due to indirect actions such as less A $\beta$  in the brain resulting in less tau kinase activation.

**Conclusions:** The significance of these findings is that DNA A $\beta$ <sub>42</sub> trimer immunotherapy targets two major pathologies in AD—amyloid plaques and neurofibrillary tangles—in one vaccine without inducing inflammatory T-cell responses, which carry the danger of autoimmune inflammation, as found in a clinical trial using active A $\beta$ <sub>42</sub> peptide immunization in patients with AD (AN1792).

**Keywords:** Alzheimer's disease, Immunotherapy, DNA vaccination, Amyloid- $\beta$ , A $\beta$  oligomer, Tau, Tau kinases

## Introduction

Immunotherapeutic approaches have high potential for successful treatment interventions in Alzheimer's disease (AD). Following the lessons learned from the first anti-amyloid- $\beta$  peptide 1–42 (anti-A $\beta$ <sub>42</sub>) clinical trial (AN1792), in which patients with AD received an A $\beta$ <sub>42</sub> vaccine and QS-21 adjuvant, which led to encephalitis in 6% of the treated patients, a major focus is now on avoiding autoimmune inflammation [1–3]. Ongoing

clinical trials are pursuing passive vaccination with mouse monoclonal antibodies (mAbs) or fully human antibodies against A $\beta$ <sub>42</sub> peptide epitopes to avoid complications from autoimmunity [4–7]. A recent study in which patients received passive immunotherapy with an mAb targeting oligomeric or prefibrillar A $\beta$ <sub>42</sub> reported positive results regarding amyloid reduction in the brain as well as improved cognitive measurements [8].

Besides amyloid accumulation, tau aggregation and spreading have been associated with progression of AD. In fact, increased tau levels showed high correlation with cognitive decline in patients with AD [9]. Tau immunotherapy is being evaluated in various preclinical and

\* Correspondence: [doris.lambracht-washington@utsouthwestern.edu](mailto:doris.lambracht-washington@utsouthwestern.edu)  
Department of Neurology and Neurotherapeutics, University of Texas Southwestern Medical Center Dallas, 5323 Harry Hines Boulevard, Dallas, TX 75390-8813, USA



clinical trials as well, using active immunizations with peptides from different parts of the tau protein or passive immunizations using polyclonal or mAbs [10–15]. Antitau antibodies have been shown to act inside and outside of neurons and to reduce tau hyperphosphorylation as well as pathogenic tau seeding [16–20].

We report, for the first time in an AD mouse model, that active DNA A $\beta_{42}$  immunization into the skin targets two pathologies: amyloid-containing plaques and tau. DNA vaccination, in which not the antigen (peptide or protein) but the DNA encoding this peptide is administered, is an alternative route of vaccination. Genes encoded by the DNA are expressed within the skin, and the peptides are taken up by dendritic cells traveling to the regional lymph nodes and presenting the antigen to B and T cells [21]. Immune responses to DNA or peptide immunization differ qualitatively. We have shown previously that full-length DNA A $\beta_{42}$  trimer immunization is noninflammatory and induces a regulatory immune response [22–25]. DNA A $\beta_{42}$  trimer immunization has been shown to be effective in removing amyloid from the brain in immunized double-transgenic mice (APPswe/PS1 [26–28]). In the present study, we used a triple-transgenic AD mouse model (3xTg-AD) that exhibits A $\beta$  and tau pathologies characteristic of human AD [29, 30]. We found that immunotherapy with DNA A $\beta_{42}$  trimer leads to reduction of A $\beta_{40}$ /A $\beta_{42}$  peptides and amyloid plaques, and we show for the first time that DNA A $\beta_{42}$  trimer immunization leads also to significant reduction of tau from the mouse brain.

## Methods

### Animals

3xTg-AD [B6;129-Tg(APPswe,tauP301L)1Lfa Psen1<sup>tm1Mpm</sup>/Mmjax, MMRRC Stock No: 34830-JAX] mice had been purchased from the Mutant Mouse Research and Resource Center at The Jackson Laboratory and were bred and housed at the UT Southwestern Medical Center animal facility under conventional conditions. This mouse model had been developed by Oddo and colleagues [29, 30]. Animal use was approved by the UT Southwestern Medical Center Animal Research Committee, and animal research was conducted under the Animal Research: Reporting of In Vivo Experiments guidelines [31].

### Study design

Cohorts of 3xTg-AD mice were immunized with a DNA A $\beta_{42}$  trimer vaccine, A $\beta_{42}$  peptide (rPeptide, Watskinville, GA, luciferase (Luc) control DNA, or left untreated as controls. This mouse model that had been developed by Oddo and colleagues develops plaque and tangle pathology [29, 30]. Cohort 1 consisted of 16 Tg female mice and 8 wild-type controls, and cohort 2 consisted of 34 Tg female mice. Parallel immunized groups of 3xTg-AD males (16 males in cohort 3, 15 males in

cohort 4) showed no plaque pathologies at 18 and 20 months of age, so this study used females only. The mice were vaccinated at a total of 13 time points until 20 months of age for final analyses. Collected brains were cut in a sagittal plane. One hemibrain was frozen and used in enzyme-linked immunosorbent assays (ELISAs) and Western blots, and the other half was fixed for immunostaining with anti-A $\beta$  and antitau antibodies.

### Immunizations and collection of blood samples

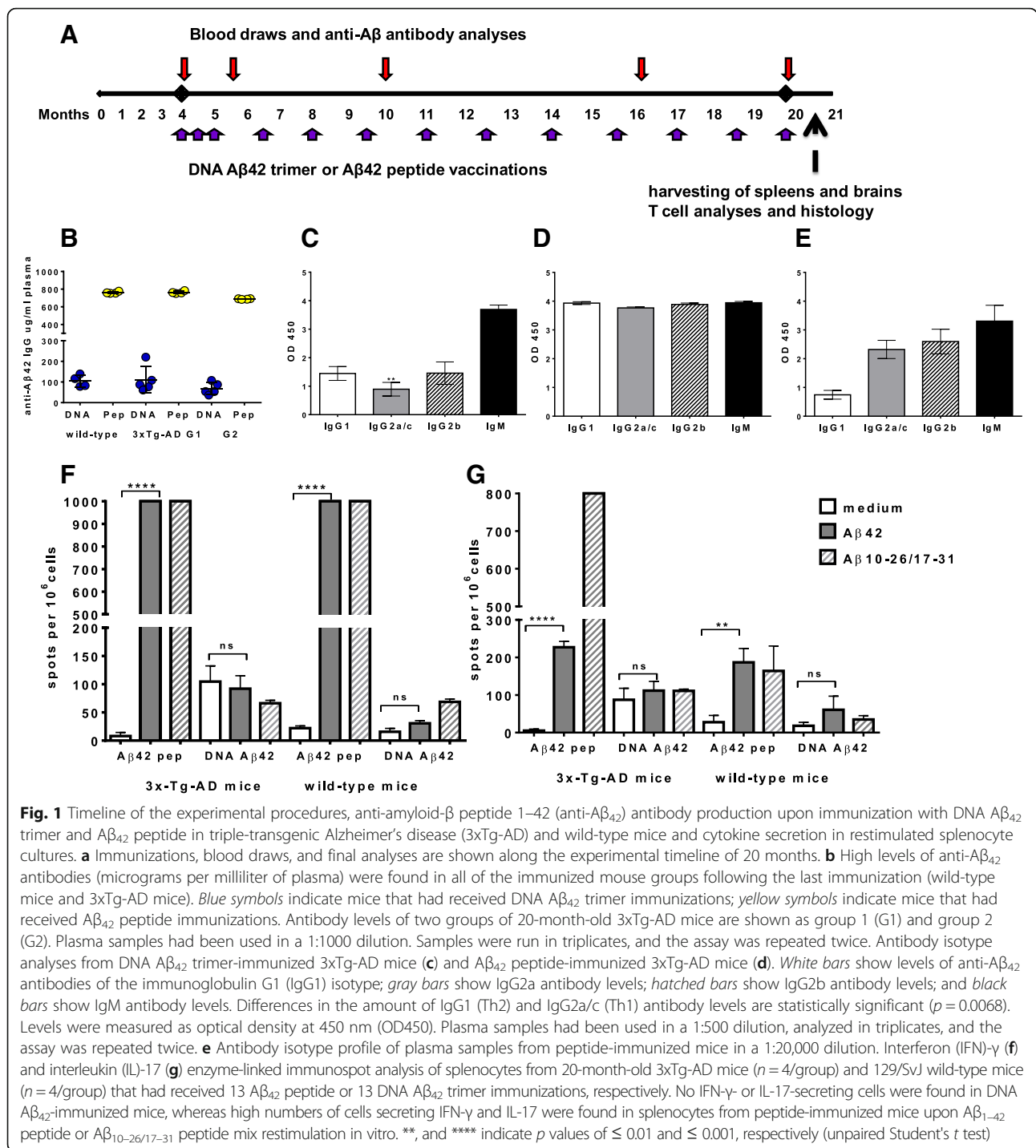
Immunizations were started in 4-month-old mice in groups of four to eight mice (3xTg-AD and 129/SvJ wild-type controls) with three initial immunizations in biweekly intervals (Fig. 1) with a Gal4/DNA A $\beta_{42}$  trimer double-plasmid system (4  $\mu$ g of DNA/immunization, ratio of 3:1 DNA A $\beta_{42}$  trimer responder plasmid/Gal4 activator plasmid) via intradermal injection using a Helios gene gun (Bio-Rad Laboratories, Hercules, CA, USA) or via intraperitoneal injections of A $\beta_{42}$  peptide (100  $\mu$ g of peptide/immunization) with Quil-A (Sigma-Aldrich, St. Louis, MO, USA) as adjuvant as previously described [22–25]. The immunizations were boosted in 6-week intervals until the mice were 18 or 20 months old (up to 13 immunizations) (Fig. 1a). Control mice received Luc DNA immunizations (group 1) or no treatment (naïve controls, group 2). Blood samples were collected at different time points throughout the study 10 days following the respective immunization time points.

### IHC of mouse brains

Sagittal parallel sections of paraformaldehyde (PFA)--fixed female mouse brains were stained with antibodies specific for A $\beta_{42}$  (6E10, BioLegend, San Diego, CA, USA; McSA1, MédiMabs, Montreal, QC, Canada; MOAB-2, MilliporeSigma, Billerica, MA, USA) to detect intraneuronal A $\beta_{42}$  deposition and amyloid plaques in the hippocampus and cortex of the mice. To stain for tangle pathology, we used HT7, AT8, AT100, AT180, and AT270 (Thermo Fisher Scientific, Waltham, MA, USA) and T22 (MilliporeSigma); anti-tau antibodies pT231, pS214, and pS404 (Abcam, Cambridge, MA, USA); and Tyr18 (MédiMabs). NeuN antibodies (clone ABN78, MilliporeSigma; clone 1B7, Abcam) were used to stain neurons. Prior to the staining, sections were treated with heat-mediated antigen retrieval for all the tau antibodies or incubation in 70% formic acid for all the A $\beta$  antibodies. After staining, tissues were scanned using a NanoZoomer digital pathology system and analyzed with NDP.view software (both from Hamamatsu Photonics, Shizuoka, Japan).

### Positive antibody staining area quantification

The A $\beta$  and tau immunoreactive areas were quantified using the “area measure” tool in ImageJ software (National Institutes of Health, Bethesda, MD, USA [32]).



Immunostained sections (sagittal sections of mouse brain) were imaged with a 20 $\times$  objective and were converted into 8-bit grayscale. The Analyze > Measure tool was used to measure the total area occupied by positive staining in each image. The total area was averaged for the sections per mouse group. Values are arbitrary units expressed as mean  $\pm$  SEM per area.

### Anti- $A\beta_{42}$ antibody ELISA and cytokine enzyme-linked immunospot assays

ELISAs for antibody levels in mouse plasma were performed according to standard procedures. Cytokine concentrations from cell culture supernatants and enzyme-linked immunospot (ELISPOT) assays to determine frequencies of cytokine-secreting cells were performed

according to standard procedures and as previously described using commercially available antibody sets for mouse interferon (IFN)- $\gamma$ , interleukin (IL)-17, and IL-4 (eBioscience, San Diego, CA, USA) [23–25].

### A $\beta$ and tau ELISAs

For semiquantitative analyses of total A $\beta_{42}$ , A $\beta_{40}$ , and tau (total tau, pT231, pS396, pT181, and pS199) levels in the brain, standard ELISAs were used (Thermo Fisher Scientific). Frozen mouse hemibrains of female mice were homogenized with a Dounce homogenizer in 10 volumes (wet brain weight) of extraction buffer [1 mM Tris, 1 mM ethylene glycol-bis( $\beta$ -aminoethyl ether)-*N,N,N',N'*-tetraacetic acid (EGTA), 1 mM dithiothreitol (DTT), 10% sucrose, pH 7.5). Following homogenization, lysates were centrifuged at 26,000  $\times g$  for 15 min at 4 °C to clear the homogenate. The supernatant (Sup 1) was removed, and the pellet was resuspended in 1% Triton<sup>®</sup> X-100/1 mM Tris/1 mM EGTA/1 mM DTT/10% sucrose, pH 7.5. The solution was centrifuged at 188,000  $\times g$  for 60 min at 4 °C. The supernatant was removed and stored at -80 °C (detergent-soluble supernatant). The pellet was washed, dried, and dissolved in 5 M guanidine (nonsoluble fraction). Lysates containing the detergent-soluble and -nonsoluble brain fractions were further diluted in homogenate assay buffer (0.2 g/L KCl, 0.2 g/L KH<sub>2</sub>PO<sub>4</sub>, 8.0 g/L NaCl, 1.15 g/L Na<sub>2</sub>HPO<sub>4</sub>, 5% bovine serum albumin [fraction V], 0.03% Tween<sup>®</sup> 20, 1 $\times$  protease inhibitor cocktail, and 1 $\times$  phosphatase inhibitor cocktail, pH 7.4). Further dilutions and ELISAs were performed according to the manufacturer's instructions.

### Western blot analysis

Soluble hemibrain lysate fractions from female mice were separated on 12% or 8–16% SDS-PAGE gels, transferred to nitrocellulose membranes (Thermo Fisher Scientific), and probed with the primary antibody overnight at 4 °C. The following antibodies were used: Tau12, 43D (BioLegend), HT7 (Thermo Fisher Scientific), anti-extracellular signal-regulated kinase 1/2 (anti-ERK1/2) and phosphorylated ERK1/2, mitogen-activated protein kinase kinase 1/2 (MEK1/2) and phosphorylated MEK1/2, GSK-3 $\beta$ , GSK-3 $\alpha$ / $\beta$ , glyceraldehyde 3-phosphate dehydrogenase (GAPDH),  $\beta$ -actin (1:1000; Cell Signaling Technology, Danvers, MA, USA), tubulin  $\beta$  (1:1000; Bio-Rad Laboratories), and phosphorylated glycogen synthase kinase 3 $\beta$  (GSK3 $\beta$ ) Y216 (1:1000; Abcam). After incubation with horseradish peroxidase-conjugated secondary antibodies (Thermo Fisher Scientific; SouthernBiotech, Birmingham, AL, USA), antibody binding was visualized with an enhanced chemiluminescence detection reagent (ProSignal ECL; Genesee Scientific, San Diego, CA, USA) and captured on a Syngene G:Box system using GeneSys software (Syngene USA, Frederick, MD, USA). Gray-level intensities (densitometries)

were quantified using gel analysis in ImageJ software [32]. For verification of similar total protein concentrations applied on the SDS-PAGE gels, filters were reprobated with housekeeping genes GAPDH, actin, and tubulin.

### Statistics

For statistical analysis (unpaired Student's *t* test with two-tailed *p* values, nonparametric Mann-Whitney *U* test, parametric multiple comparisons one-way analysis of variance [ANOVA] and column statistics), Prism software version 6 for Windows (GraphPad Software, La Jolla, CA, USA) was used. *p*  $\leq$  0.05 was considered significant.

## Results

### Humoral and cellular immune responses in A $\beta_{42}$ -immunized mice

In 20-month-old transgenic mice that had received 13 immunizations (Fig. 1a), antibody levels reached 69.88  $\pm$  11.08  $\mu$ g of anti-A $\beta_{42}$  immunoglobulin G (IgG)/ml of plasma (63.77  $\pm$  19.53  $\mu$ g anti-A $\beta_{42}$  IgG/ml plasma in group 2) after DNA A $\beta_{42}$  immunization and 655.9  $\pm$  9.58  $\mu$ g/ml after A $\beta_{42}$  peptide immunization (763.4  $\pm$  11.88  $\mu$ g anti-A $\beta_{42}$  IgG/ml plasma in group 2). Similar antibody levels were found in parallel immunized 20-month-old wild-type control animals: 49.79  $\pm$  6.35  $\mu$ g/ml in DNA A $\beta_{42}$ -immunized mice and 659.7  $\pm$  6.95  $\mu$ g/ml in A $\beta_{42}$  peptide-immunized mice (Fig. 1b). DNA A $\beta_{42}$  trimer-immunized mice had high levels of IgG1 and IgG2b antibodies. The overall isotype composition was IgG1 = IgG2b > IgG2a/c (IgG1/IgG2a ratio of 1.61). Low levels of IgG2a/c antibodies were consistent with a noninflammatory Th2 immune response (Fig. 1c). All peptide-immunized mice had mixed isotype profiles with similar levels of IgG1, IgG2a/c, and IgG2b antibodies, indicative of a mixed Th1/Th2 immune response (Fig. 1d). This mixed profile was found at high plasma dilutions up to 1:20,000 (Fig. 1e).

ELISPOT assays from splenocyte cultures of 3xTg-AD mice and wild-type mice were performed to detect IFN- $\gamma$  (Th1 cytokine), IL-17A (Th17 cytokine), and IL-4 (Th2 cytokine) upon A $\beta_{42}$  peptide restimulation in the immunized mice. Although we found high numbers of IFN- $\gamma$ - and IL-17-secreting cells in peptide-immunized mice, low numbers of cells secreting these proinflammatory cytokines were found in DNA-immunized mice. In peptide immunized 3xTg-AD mice, IFN- $\gamma$ -secreting cells were detected with 8  $\pm$  11.27 spots in medium control wells and more than 1000 spots in the A $\beta_{42}$  peptide restimulated wells (*p* < 0.0001 by Mann-Whitney *U* test) (Fig. 1f). We counted 104.7  $\pm$  47.9 spots in medium control wells of DNA A $\beta_{42}$ -immunized 3xTg-AD mice with no increase in peptide restimulated wells (92  $\pm$  39.95 spots; *p* = 0.7428). A similar pattern was observed for IL-17-secreting cells with increased numbers in A $\beta_{42}$

peptide-immunized mice:  $227 \pm 15.52$  spots after peptide restimulation compared with  $5.3 \pm 4.04$  spots in medium control wells ( $p < 0.0001$  by Mann Whitney *U* test) and no significant increase in IL-17-secreting cells after peptide restimulation in DNA A $\beta_{42}$ -immunized mice ( $87.33 \pm 30.6$  spots in A $\beta_{42}$  peptide-containing wells,  $111.7 \pm 24.58$  spots in medium control wells;  $p = 0.3439$ ) (Fig. 1g). For a peptide mix (A $\beta_{10-26}$ /A $\beta_{17-31}$ ) containing the T-cell epitope of several mouse major histocompatibility complex haplotypes ( $H2^b$ ,  $H2^k$ ,  $H2^d$ ,  $H2^s$ ), similar results were obtained in the ELISPOT assays (Fig. 1f).

### Histology showing amyloid reduction from brain

In the initial studies, we used male and female mice and found large differences in the pathology between sexes. Figure 2a–d shows sections of 18- and 20-month-old mice for comparison of A $\beta_{42}$  pathology in females and males. In 20-month-old mice, large numbers of A $\beta$  plaques were found in the subiculum of the hippocampus in female mice (Fig. 2a), whereas no plaques were found in the 20-month-old males (Fig. 2b). Also, for tau antibody staining (HT7, AT180) in parallel sections, much less pathology was found in male mice (data not shown), and therefore we continued immunotherapy in the following groups only in females. In 18-month-old mice, amyloid plaques were abundant in the female mice (Fig. 2c). In age-matched male mice, only a few neurons with intracellular A $\beta_{42}$  staining were found, but no plaques (Fig. 2d).

A $\beta_{42}$  immunotherapy led to a reduction of the number of amyloid plaques in the hippocampus of treated mice. In Fig. 2e–h, staining for NeuN, which stains neurons (red color), and an A $\beta$  antibody (McSA1), which stains amyloid plaques (brown color) are shown for the hippocampal area for representative examples of the different mouse groups in one experimental cohort. The mAb McSA1 recognizes the N-terminal region of the human A $\beta$  peptide (A $\beta_{1-12}$ ). This epitope is present in  $\beta$ -C-terminal fragment and amyloid precursor protein (APP) as well, but McSA1 has been reported as highly specific for A $\beta$  as opposed to APP or soluble APP following competition studies with these antigens [33, 34]. Figure 2e shows staining of the hippocampus subiculum of a 20-month-old 3xTg-AD control female mouse. Figure 2f shows this area stained for neurons and amyloid in a 20-month-old wild-type control mouse. A reduction of amyloid plaques was seen in all mice that had received A $\beta$  immunotherapy. Representative sections are shown for one A $\beta_{42}$  peptide-immunized mouse (Fig. 2g) and one DNA A $\beta_{42}$ -immunized 3xTg-AD mouse (Fig. 2h).

Immunohistological staining of plaques in the brains of these mice was subjected to the counting of plaques  $> 10 \mu\text{m}$  in corresponding  $1\text{-mm}^2$  areas (subiculum/CA1) of 15 control mice (7 DNA A $\beta_{42}$ -immunized mice and 8 A $\beta_{42}$  peptide-immunized mice) by two blinded

experimenters. These analyses showed significantly reduced plaque numbers in the DNA A $\beta_{42}$ -immunized mice ( $p = 0.0238$  by Student's *t* test compared with control mice) and a nonsignificant reduction in the A $\beta_{42}$  peptide-immunized mice ( $p = 0.6809$ ). Also, the difference in plaque numbers between the DNA A $\beta_{42}$ - and peptide-immunized mice was significant ( $p = 0.0487$ ) (Fig. 2i).

### Histology showing reduction in levels of phospho-tau

The use of the 3xTg-AD mouse model allowed us to analyze a second pathology of human AD, which is the hyperphosphorylation of tau and development of neurofibrillary tangles. IHC of 3xTg-AD brain sections with different antibodies specific for tau molecules phosphorylated at specific residues (AT180, AT8, AT270, pT404, pS212, Tyr18) showed that A $\beta_{42}$  immunotherapy also led to a significant reduction in the levels of tau phosphorylation. In Fig. 3a, the age progression for tau phosphorylation in the 3xTg-AD mouse model is shown. Brains from 2-, 4-, 7-, 9-, 12-, and 18-month-old mice ( $n = 4/\text{group}$ ) were harvested, and PFA-fixed, paraffin-embedded sections were analyzed with the mAb AT180, which detects tau phosphorylated at residue T231. In the comparison of the staining pattern with brains from 18-month-old 3xTg-AD mice, which had received DNA A $\beta_{42}$  immunizations, we observed that the AT180 staining intensity of the immunized 18-month-old mice appeared more like the staining intensity in brains from 7- or 9-month-old mice (Fig. 3b). Sections from four 18-month-old Luc immunized control mice, five 18-month-old DNA A $\beta_{42}$ -immunized mice, and six 18-month-old A $\beta_{42}$  peptide-immunized mice were semi-quantitatively analyzed with the area measure tool in ImageJ software. The results showed an about 40% reduction after DNA A $\beta_{42}$  immunization and an approximately 20% reduction after A $\beta_{42}$  peptide immunization (Fig. 3c). However, owing to high SDs and the small number of control animals, the results were not statistically significant.

Staining with the AT8 antibody specific for pS201/pT205, which is a late tau phosphorylation site [35], was less prominent in 18-month-old mice, but good staining was observed in 20-month-old mice, which showed reduction of AT8 staining in DNA A $\beta_{42}$  trimer-immunized mice. Figure 3d shows that AT8-positive neurons were detected in the hippocampus of 20-month-old 3xTg-AD control mice (sections from two mice). Two representative sections from the A $\beta_{42}$  peptide-immunized 20-month-old 3xTg-AD mice are shown in Fig. 3e. The brains showed fewer AT8-positive neurons than in the control animals. Much less staining was found in DNA A $\beta_{42}$  trimer-immunized mice. Figure 3 shows the respective brain sections of the hippocampus from two mice (insets show higher magnification of subiculum in Fig. 3f).

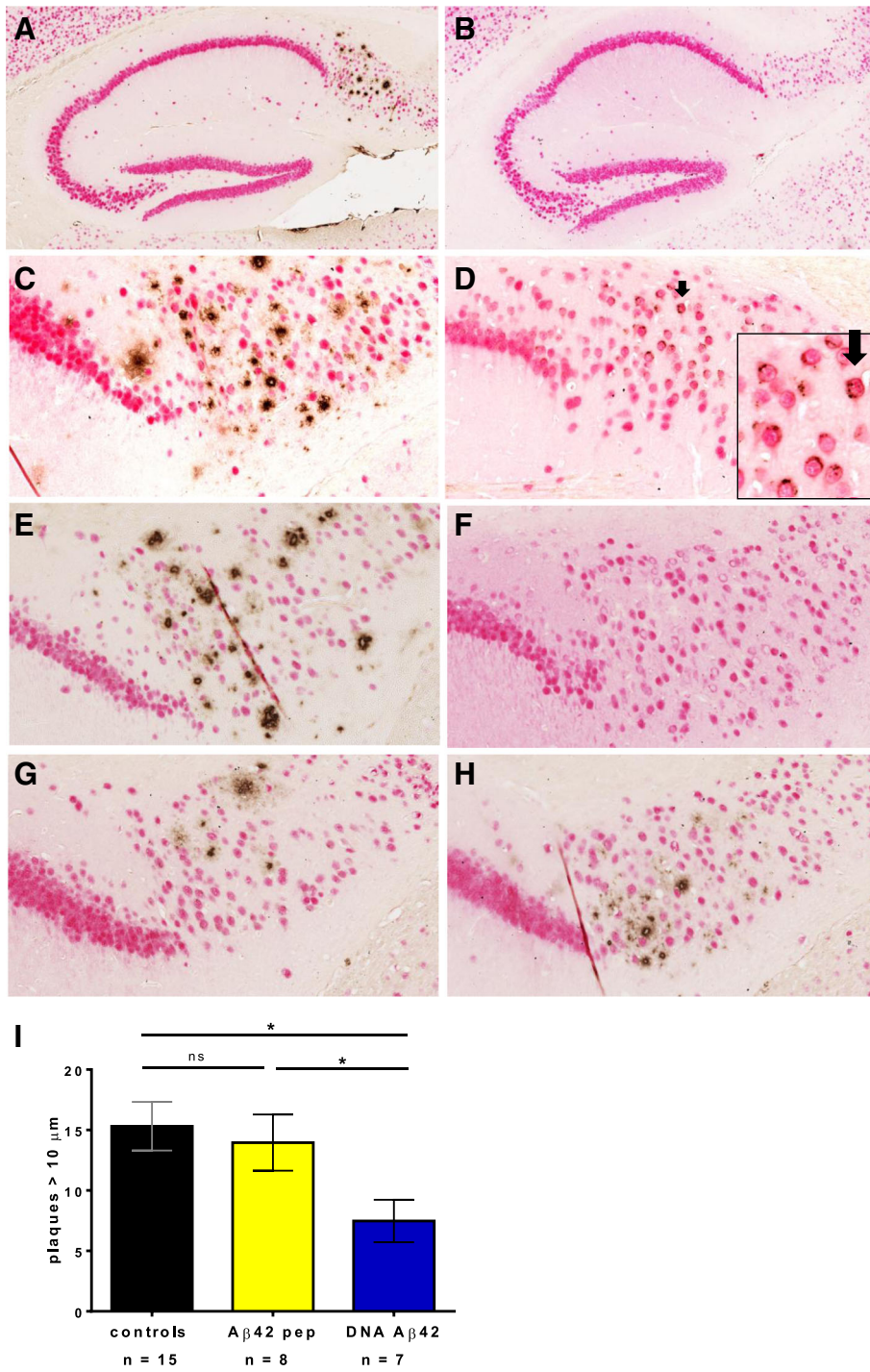


**Fig. 2** (See legend on next page.)

(See figure on previous page.)

**Fig. 2** Amyloid- $\beta$  ( $A\beta$ ) immunization results in removal of amyloid plaques in brains of triple-transgenic Alzheimer's disease (3xTg-AD) mice. Brain sections of mice aged 18 months (**c** and **d**) and 20 months (**a**, **b**, **e-h**) were stained with a NeuN antibody (*red*) to detect neurons and an anti- $A\beta$  antibody (McSA1, *brown*) to detect numerous plaques in the subiculum of the hippocampus in 3xTg-AD mice. **a** The hippocampus of a 20-month-old female control 3xTg-AD mouse with numerous amyloid plaques is shown (5x magnification). **b** Hippocampus of a 20-month-old male control 3xTg-AD mouse showing no plaque pathology. **c** The subiculum of an 18-month-old female control 3xTg-AD mouse is shown at higher magnification (20x). **d**  $A\beta$  staining in the subiculum of an 18-month-old male mouse. Only intraneuronal  $A\beta$  can be detected (indicated with *arrow* and shown at higher magnification in *inset*). **e** Numerous plaques in the hippocampus of an untreated 20-month-old 3xTg-AD female mouse. **f** No plaques were found in 20-month-old wild-type mice. Both immunization regimens,  $A\beta_{42}$  peptide (**g**) and DNA  $A\beta_{42}$  (**h**), led to a reduction of plaques in 20-month-old 3xTg-AD mice compared with the control mouse (**e**). **i** Images were counted for plaques  $\geq 10 \mu\text{m}$  in a  $1\text{-mm}^2$  area of the subiculum/CA1 of the hippocampus by two blinded experimenters. *Blue bars* show plaque count in DNA  $A\beta_{42}$  trimer-immunized mice ( $n = 7$ ), and *yellow bars* show plaque count found in brains of  $A\beta_{42}$  peptide-immunized mice ( $n = 8$ ). *Black bars* show the numbers found in age- and gender-matched 3xTg-AD control mice ( $n = 15$ ). \* indicates  $p$  value of  $\leq 0.05$  (unpaired Student's  $t$  test)

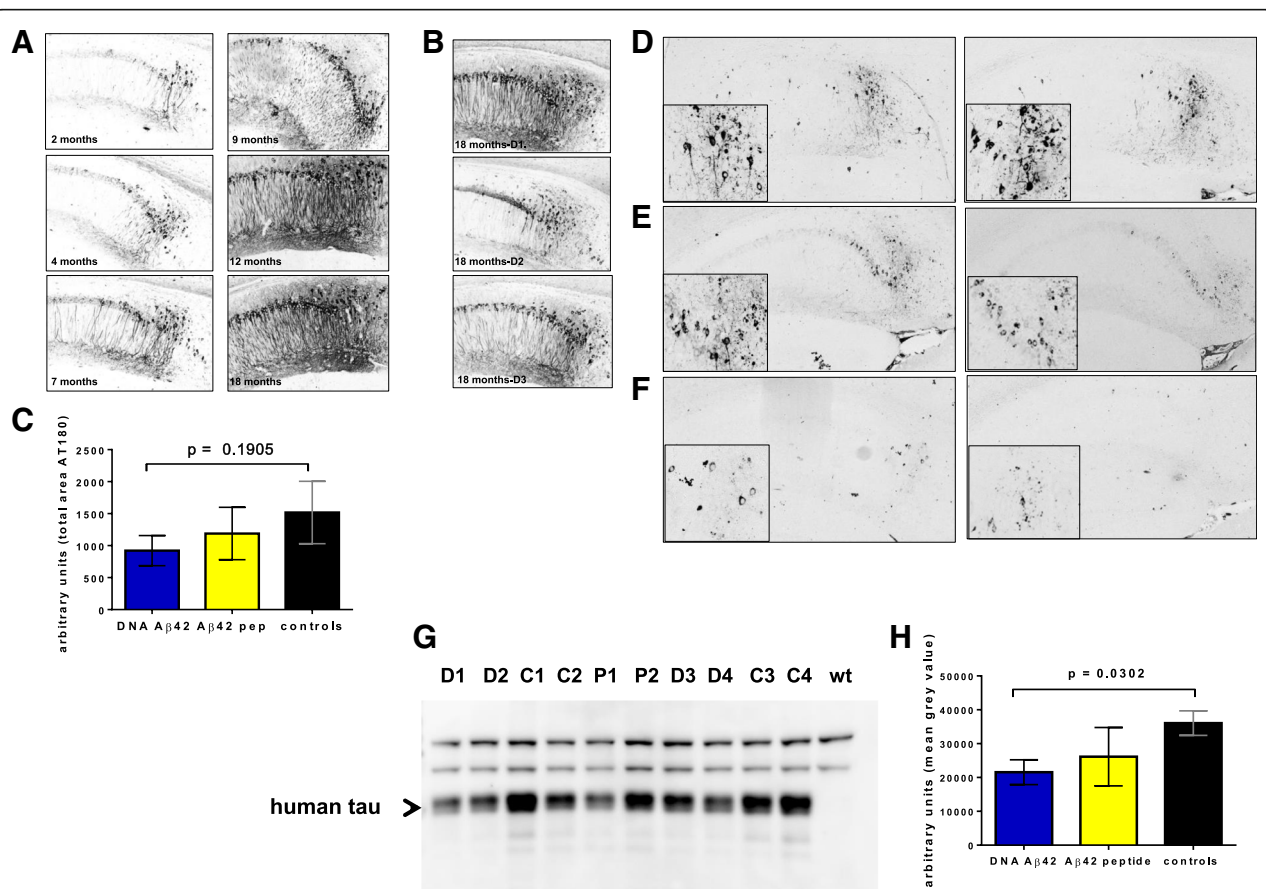


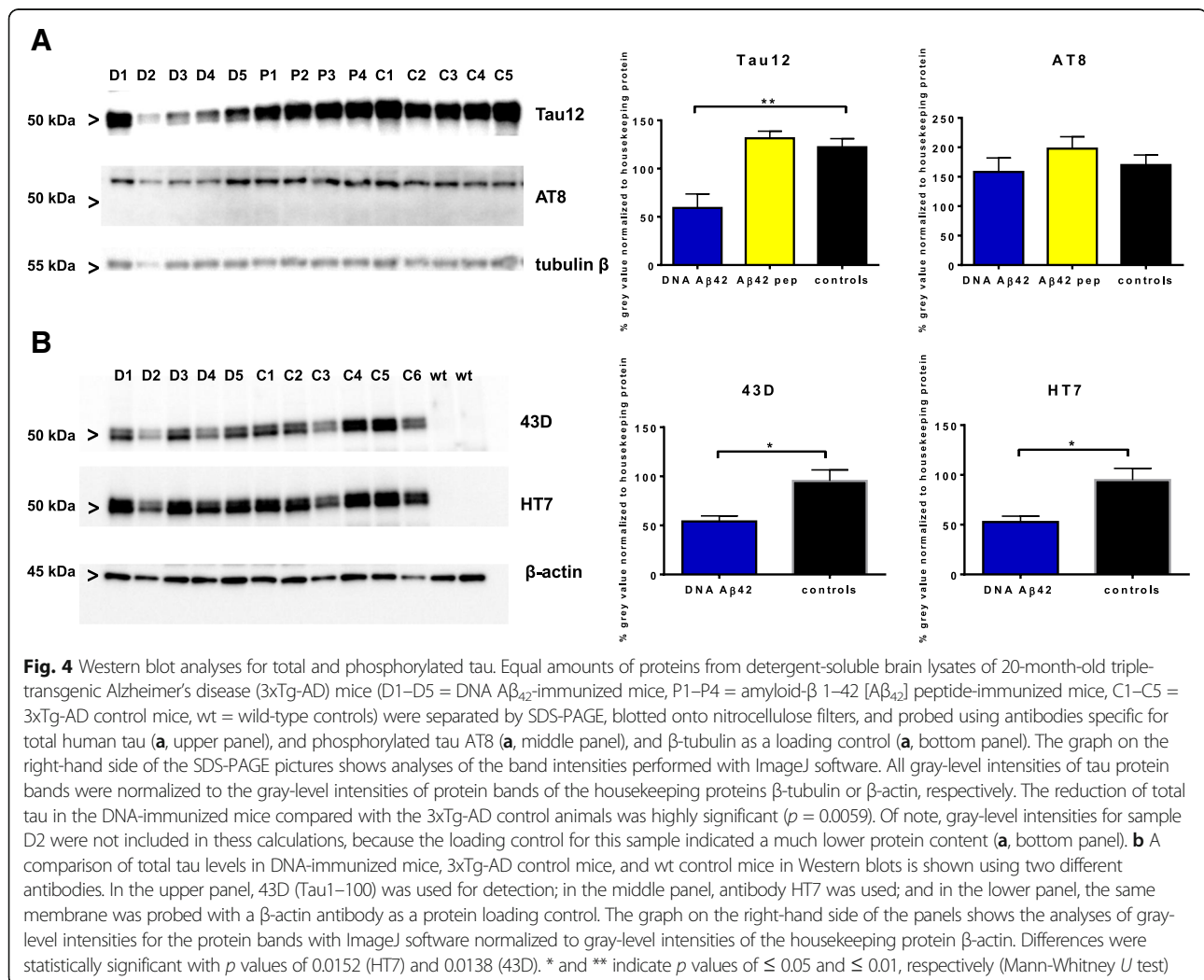
**Fig. 3** IHC staining of T231p (AT180) and T202p/S205p (AT8) in triple-transgenic Alzheimer's disease (3xTg-AD) mouse brains and Western blots for total tau. **a** The age progression of T231p (AT180) in 3xTg-AD mouse brains is shown by IHC and staining in 2-, 4-, 7-, 9-, 12-, and 18-month-old mice. **b** T231p staining in the hippocampus of three brains from 18-month-old 3xTg-AD mice that had received DNA amyloid- $\beta$  1-42 peptide ( $A\beta_{42}$ ) trimer immunizations is shown for comparison. **c** Semiquantitative analyses for pT231 staining in the hippocampus of four 18-month-old control mice, five 18-month-old DNA  $A\beta_{42}$  immunized mice, six 18-month-old  $A\beta_{42}$  peptide-immunized mice, and four wild-type mice using ImageJ software (National Institutes of Health, Bethesda, MD, USA). *Blue bars* show positive areas found in DNA  $A\beta_{42}$  trimer-immunized mice, and *yellow bars* show areas found in brains of  $A\beta_{42}$  peptide-immunized mice. *Black bars* show the values of age- and gender-matched 3xTg-AD control mice. **d-f** DNA  $A\beta_{42}$  trimer immunization decreased AT8 staining in hippocampal sections from 20-month-old 3xTg-AD mice. **d** Representative sections from two control mice. **e** Sections from  $A\beta_{42}$  peptide-immunized mice. **f** Staining of AT8<sup>+</sup> tangles in the hippocampus of two DNA  $A\beta_{42}$ -immunized mice. All pictures are in 10x magnification (hippocampus); *insets* are in 40x magnification (subiculum). **g** A representative Western blot from detergent-soluble brain lysates of 20-month-old 3xTg-AD control mice (labeled C1-C4), DNA  $A\beta_{42}$ -immunized mice (labeled D1-D4),  $A\beta_{42}$  peptide-immunized mice (labeled P1, P2), and a wild-type control (wt) mouse is shown. **h** Gray value intensities of human tau bands (indicated with an *arrowhead*, missing in the wt control, at 50 kD) were semiquantitatively analyzed using ImageJ software. *Black bars* show the values in 3xTg-AD control mice; *yellow bars* represent the peptide-immunized mice; and *blue bars* show values found in DNA  $A\beta_{42}$ -immunized mice

The histological data indicating a possible reduction of tau in the A $\beta_{42}$ -immunized mice led to further substantiation of this finding by Western blot analysis and a panel of commercially available tau ELISAs that allowed testing for statistical significance of reduction of different tau phosphorylation patterns.

#### Western blot analysis of total tau

The reduction of tau in mice that had received A $\beta_{42}$  immunotherapy was further analyzed using Western blotting of the brain lysates. In the comparison of total tau detected with the mAb Tau12, it was found that both immunotherapies led to a reduction in tau. The reduction was not significant in A $\beta_{42}$  peptide-immunized mice and was higher and significant in DNA A $\beta_{42}$ -immunized mice ( $p$  values of 0.0302, 0.0142, and 0.0023 from three independently performed Western blot analyses with detergent-soluble brain lysates). Figure 3g and h shows the results of one of these experiments (Western blot and ImageJ analysis of gray-level intensities of the bands,

respectively). Total tau and phosphorylated tau were further analyzed by Western blotting, and the results are shown in Fig. 4. All band intensities were normalized to band intensities found in the reprobing of the Western blots with antibodies to housekeeping proteins. In the detergent-soluble fractions, tau detected with the mAb Tau12 was significantly reduced in brain lysates from DNA A $\beta_{42}$ -immunized mice ( $p = 0.0059$  by Student's unpaired  $t$  test) (Fig. 4a). The intensity of the Western blot band reactive to the mAb AT8 was only slightly reduced in DNA A $\beta_{42}$ -immunized mice ( $p = 0.3224$ , nonsignificant). The AT8-reactive protein band was found at higher molecular weight (about 65 kDa), which might correspond to the 64 kDa tau, a Tris-buffered saline-extractable hyperphosphorylated tau species described in the rTg4510 mouse brain (Fig. 4a, middle panel) [36]. In Fig. 4b, two different total human tau antibodies, 43D and HT7, were directly compared in parallel-run SDS-PAGE. Significant reductions of tau were found in the brain samples from DNA



A $\beta_{42}$ -immunized mice (HT7 antibody,  $p = 0.0152$ ; 43D antibody,  $p = 0.0138$ ).

These results are consistent with the ELISA results described in the "Quantification of tau in ELISAs" section below. Although the reductions in the detergent-soluble brain lysate fractions were obvious but statistically not significant, reductions in the nonsoluble brain lysates were highly significant. However, the nonsoluble fractions could not be tested, owing to the extraction method used with 5 M guanidine for the solubilization of the pellet. These samples are not compatible with SDS-PAGE. In future mouse cohorts, we will use a different extraction protocol allowing the nonsoluble brain lysate fractions to be analyzed in Western blots (SDS-PAGE).

#### Quantification of A $\beta_{x-42}$ and A $\beta_{x-40}$ in ELISAs

After analysis of brain histology as shown in Fig. 2, ELISAs were used for semiquantitative analyses of reduction of A $\beta_{x-40}$  and A $\beta_{x-42}$  peptides in DNA A $\beta_{42}$  trimer- and A $\beta_{42}$  peptide-immunized female 3xTg-AD mice. An increase of A $\beta_{42}$  and A $\beta_{40}$  peptides in brains from 3xTg-AD mice with age is shown in Fig. 5a. ELISAs were also used to quantify the reduction of A $\beta_{x-40}$  and A $\beta_{x-42}$  peptides due to DNA A $\beta_{42}$  trimer and A $\beta_{42}$  peptide immunization (Fig. 5b and c). Statistical significance for reduction of A $\beta_{42}$  and A $\beta_{40}$  was reached in the comparison of DNA A $\beta_{42}$  trimer-immunized mice ( $n = 7$ , blue bars) compared with control animals ( $n = 14$ , black bars) in the nonsoluble fractions ( $p = 0.0461$ , Mann-Whitney  $U$  test, for A $\beta_{x-42}$ ;  $p = 0.0125$  for A $\beta_{x-40}$ ). These reductions were nonsignificant in the one-way ANOVA (Fig. 5b). In the soluble brain lysate fractions, a reduction of both A $\beta$  peptides was highly significant ( $p < 0.0008$ , Mann-Whitney  $U$  test;  $p = 0.0123$ , one-way-ANOVA, for A $\beta_{x-42}$ ;  $p = 0.0017$ , Mann-Whitney  $U$  test;  $p = 0.0028$ , one-way ANOVA for A $\beta_{x-40}$ ) (Fig. 5c) in DNA A $\beta_{42}$ -immunized mice. A $\beta_{x-42}$  peptides were also reduced in brains from A $\beta_{42}$  peptide-immunized 3xTg-AD mice in the nonsoluble lysate and detergent-soluble lysates, but levels did not reach statistical significance ( $p = 0.2766$  for nonsoluble A $\beta_{x-42}$ ,  $p = 0.0815$  for soluble A $\beta_{x-42}$ ). Much less removal was found for A $\beta_{x-40}$  peptides in brains from A $\beta_{42}$  peptide-immunized mice (Fig. 5b and c, yellow bars, right-hand graphs).

#### Quantification of tau in ELISAs

Histological analyses of the mouse brains with tau antibodies AT180 and AT8 (early and late tau phosphorylation) showed reduced staining in the immunized mice (Fig. 3). ELISAs were used for detection of total tau, pT231 tau, p396 tau, pT181 tau, and pS199 tau in the semiquantitative analyses of tau reduction in DNA A $\beta_{42}$  trimer- and A $\beta_{42}$  peptide-immunized 3xTg-AD mice. Tau was reduced in

both mouse groups, which had received A $\beta_{42}$  immunotherapy or DNA or peptide vaccine (Fig. 6a–e, Table 1). However, statistical significance was reached only in the DNA A $\beta_{42}$  trimer-immunized mice (Table 1).

High levels of tau protein were found in the detergent soluble fractions:  $1.235 \times 10^5 \pm 0.556 \times 10^5$  pg/ml brain lysate in the 20-month-old female 3xTg-AD control mice ( $n = 14$ ), with small reductions in the mouse groups that had received A $\beta_{42}$  immunotherapy ( $1.201 \times 10^5 \pm 0.44 \times 10^5$  pg/mg in the peptide-immunized mice [ $p = 0.9754$ ,  $n = 9$ ], and  $0.928 \times 10^5 \pm 0.324 \times 10^5$  pg/mg [ $p = 0.1285$ ] in DNA-immunized mice [ $n = 7$ ]). Higher reductions of total tau were found in the nonsoluble brain lysate fractions: control mice had mean values of  $7.322 \times 10^5 \pm 3.301 \times 10^5$  pg/mg; A $\beta_{42}$  peptide-immunized mice had levels of  $6.879 \times 10^5 \pm 3.153 \times 10^5$  pg/mg brain weight ( $p = 0.8446$ ); and DNA A $\beta_{42}$  trimer-immunized mice had significantly reduced levels of  $3.793 \times 10^5 \pm 1.096 \times 10^6$  pg/mg brain weight of total human tau ( $p = 0.0411$ , one-way ANOVA) (Fig. 6a).

pT231 tau reached mean values of  $1793 \pm 490.3$  U/mg brain weight in the detergent-soluble brain lysate fractions of 3xTg-AD control mice,  $1454 \pm 390.6$  U/mg in A $\beta_{42}$  peptide-immunized mice, and  $1199 \pm 221.5$  U/mg in DNA A $\beta_{42}$  trimer-immunized mice. Although the reduction in the peptide-immunized mice was not significant ( $p = 0.4767$ ), the reduction in DNA-immunized mice was highly significant ( $p = 0.0091$ ). In the nonsoluble brain fractions, a mean value of  $1.296 \times 10^5 \pm 0.282 \times 10^5$  U/mg pT231 tau was found for control mice,  $1.313 \pm 0.338 \times 10^5$  U/mg was found in peptide-immunized mice, and  $0.809 \times 10^5 \pm 0.192 \times 10^5$  U/mg was found in DNA-immunized mice (Fig. 6b). Thus, A $\beta$  immunotherapy reduced the nonsoluble pT231 only in DNA A $\beta_{42}$  trimer-immunized mice ( $p = 0.0017$ ).

pS396 tau was slightly reduced in the detergent-soluble fraction for DNA A $\beta_{42}$  trimer- and A $\beta_{42}$  peptide-immunized female mice compared with 3xTg-AD female control mice ( $889.2 \pm 273.2$  pg/mg,  $1264 \pm 389.1$  pg/mg, and  $1441 \pm 566$  pg/mg, respectively;  $p = ns$  by one-way ANOVA). pS396 was significantly reduced in DNA A $\beta_{42}$  trimer-immunized mice in the nonsoluble fractions with mean levels of  $0.631 \times 10^5 \pm 0.121 \times 10^5$  pg/mg ( $p = 0.0007$ ) compared with  $1.136 \times 10^5 \pm 0.272 \times 10^5$  pg/mg in the 3xTg-AD control mice (Fig. 6c).

For pT181 tau, mean levels of  $3.869 \times 10^4 \pm 1.774 \times 10^4$  pg/mg in the detergent-soluble brain lysates of 3xTg-AD control mice were reduced to  $3.098 \times 10^4 \pm 0.99 \times 10^4$  pg/mg in A $\beta_{42}$  peptide-immunized mice ( $p = 0.3686$ ) and to  $1.969 \times 10^4 \pm 0.507 \times 10^4$  pg/mg in DNA A $\beta_{42}$  trimer-immunized mice ( $p = 0.0198$ ). In the nonsoluble brain fractions, a level of  $1.876 \times 10^5 \pm 0.591 \times 10^5$  pg/mg was measured for female 3xTg-AD control mice, which was reduced to  $1.672 \times 10^5 \pm 0.661 \times 10^5$  pg/mg ( $p = 0.5123$ ) in A $\beta_{42}$  peptide-immunized mice and to  $0.911 \times 10^5 \pm 0.248 \times 10^5$  pg/mg

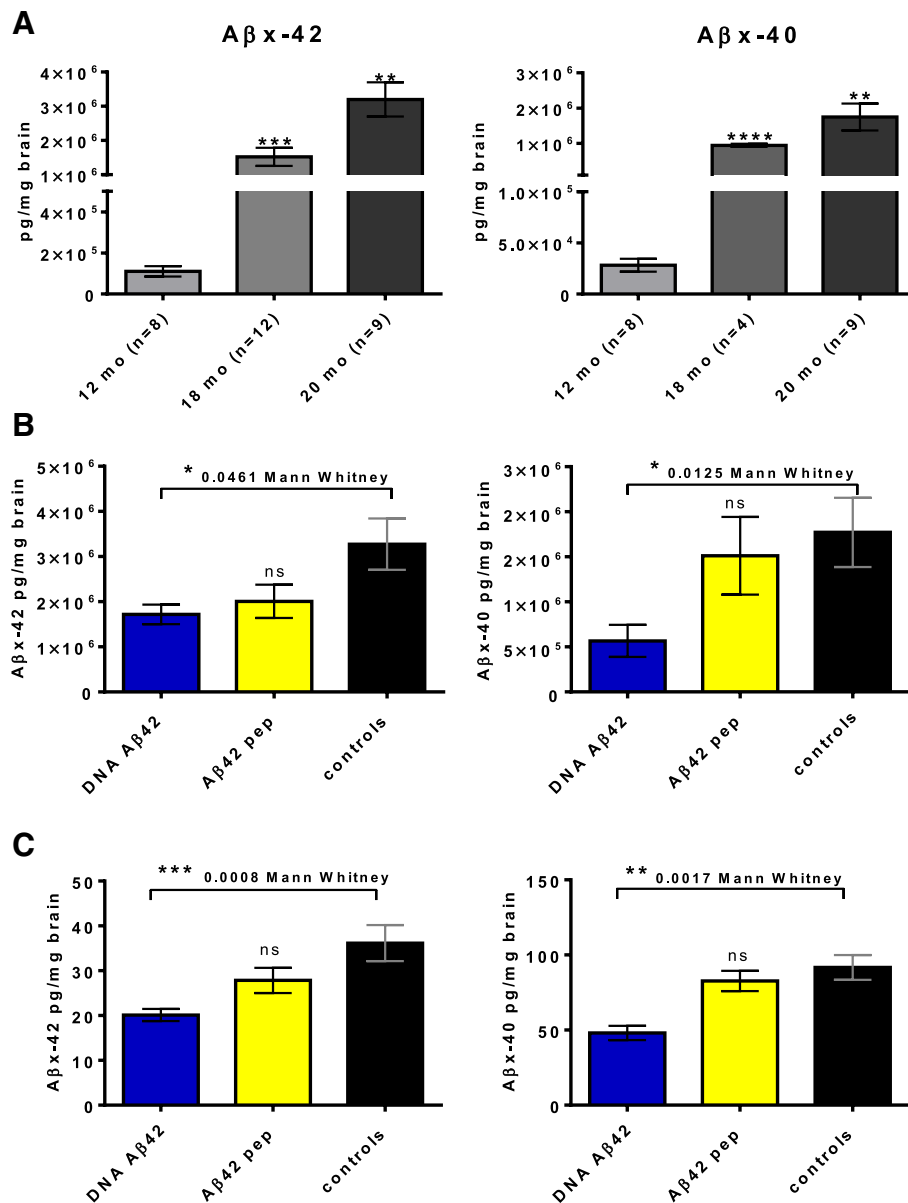


**Fig. 5** Quantitative enzyme-linked immunosorbent assay (ELISA) analyses for amyloid-β 1–42 peptide (Aβ<sub>42</sub>) and Aβ<sub>40</sub> in brain lysates from triple-transgenic Alzheimer's disease (3xTg-AD) mice. **a** Analyses of an increase of Aβ<sub>42</sub> and Aβ<sub>40</sub> peptides in brains from 3xTg-AD mice with age (12-month-, 18-month-, and 20-month-old female control mice). **b** Reduction of Aβ<sub>42</sub> and Aβ<sub>40</sub> peptide concentrations in the nonsoluble fractions of the brain lysates owing to Aβ<sub>42</sub> immunotherapy. *Blue bars* show Aβ<sub>42</sub> peptide concentrations found in brains from DNA Aβ<sub>42</sub> trimer-immunized mice; *yellow bars* show the concentrations found in brains from Aβ<sub>42</sub> peptide-immunized mice. The *black bars* show Aβ<sub>42</sub> peptide concentrations in age- and gender-matched 3xTg-AD control mice. The left-hand graph displays data for Aβ<sub>42</sub> peptides, and the right-hand graph shows data for Aβ<sub>40</sub> peptides. **c** Reduction of Aβ<sub>42</sub> and Aβ<sub>40</sub> peptide concentrations in the soluble fractions of the brain lysates owing to Aβ<sub>42</sub> immunotherapy. The left-hand graph shows data for Aβ<sub>42</sub> peptides, and the right-hand graph displays data for Aβ<sub>40</sub> peptides. ELISAs for the nonsoluble brain lysates were performed three times (dilution 1:10,000), and ELISAs for the detergent-soluble brain lysates were performed twice (dilution 1:2) for this particular group of mice and confirmed the data shown. \*  $p \leq 0.05$ , \*\*  $p \leq 0.01$ , \*\*\*  $p \leq 0.005$ , and \*\*\*\*  $p \leq 0.001$  (Mann-Whitney  $U$  test)

( $p = 0.002$ , one-way ANOVA) in DNA Aβ<sub>42</sub> trimer-immunized 3xTg-AD mice (Fig. 6d).

pS199 tau was also reduced after DNA Aβ<sub>42</sub> immunotherapy: 20-month-old 3xTg-AD control mice had a mean  $5341 \pm 1208$  pg/mg wet brain weight in the detergent-soluble fractions, and DNA Aβ<sub>42</sub> trimer-immunized mice had a

reduced level of  $3227 \pm 730.5$  pg/mg wet brain weight ( $p = 0.0012$ ). Aβ<sub>42</sub> peptide-immunized mice showed no reduction ( $5094 \pm 1246$  pg/mg,  $p = 0.5995$ ). Significant differences were present in the nonsoluble brain lysate fractions between female control and DNA Aβ<sub>42</sub> trimer-immunized mice with mean levels of  $2.69 \times 10^5 \pm 5.46 \times 10^4$  pg/mg in

**Table 1** Tau reductions in 20-month-old female 3xTg-AD mice following A $\beta$ 42 immunotherapy

	Non-soluble fraction				Detergent soluble fraction					
	DNA A $\beta$ 42 vaccine Comparison to control mice		A $\beta$ 42 pep vaccine Comparison to control mice		Comparison DNA and peptide vaccine	DNA A $\beta$ 42 vaccine Comparison to control mice		A $\beta$ 42 pep vaccine Comparison to control mice		Comparison DNA and peptide vaccine
	% tau reduction	<i>p</i> value	% tau reduction	<i>p</i> value	<i>p</i> value	% tau reduction	<i>p</i> value	% tau reduction	<i>p</i> value	<i>p</i> value
Total tau human	- 49%	<b>0.0087**</b>	- 7%	0.8446	<b>0.0418*</b>	- 25%	0.1285	- 3%	0.9754	0.2523
pT231 (AT180)	- 37%	<b>0.0008***</b>	no reduction	0.8291	<b>0.0164*</b>	- 33%	<b>0.0016**</b>	- 19%	0.4767	0.1142
pS396 (PHF)	- 44%	<b>0.0001***</b>	- 7%	0.4312	<b>0.0059**</b>	- 39%	<b>0.0097**</b>	- 12%	0.8775	<b>0.0311*</b>
pT181 (AT270)	- 51%	<b>0.0008***</b>	- 11%	0.5123	<b>0.0115*</b>	- 49%	<b>0.0005****</b>	- 20%	0.3686	0.0712
pS199	- 42%	<b>&lt; 0.0001****</b>	- 13%	0.2496	<b>0.0164*</b>	- 40%	<b>0.0002****</b>	- 5%	0.5995	<b>0.0115*</b>

Bold letters indicate differences higher than 20% in DNA A $\beta$ 42 trimer immunized mice compared to A $\beta$ 42 peptide immunized mice; letters in bold cursive font indicate high significance for differences in reduction of tau in DNA A $\beta$ 42 trimer and A $\beta$ 42 peptide immunized mice compared to the control mice, and in the comparison of the two immunization groups (Mann Whitney *u* test).

\* indicates *p* values  $\leq 0.05$ , \*\* indicates *p* values  $\leq 0.005$ , \*\*\* indicates *p* values  $\leq 0.001$ , and \*\*\*\* indicates *p* values  $< 0.0001$ . All data are based on the analyses and comparison of seven DNA A $\beta$ 42 trimer immunized mice, nine A $\beta$ 42 peptide immunized mice, and 14 age and gender matched 3xTg-AD control mice

control mice and  $1.58 \times 10^5 \pm 2.32 \times 10^4$  pg/mg in DNA-immunized mice ( $p = 0.0007$ ) (Fig. 6e, Table 1). In peptide-immunized mice the reduction was not significant, with  $2.34 \times 10^5 \pm 6.86 \times 10^4$  pg pS199/mg ( $p = 0.2496$ ).

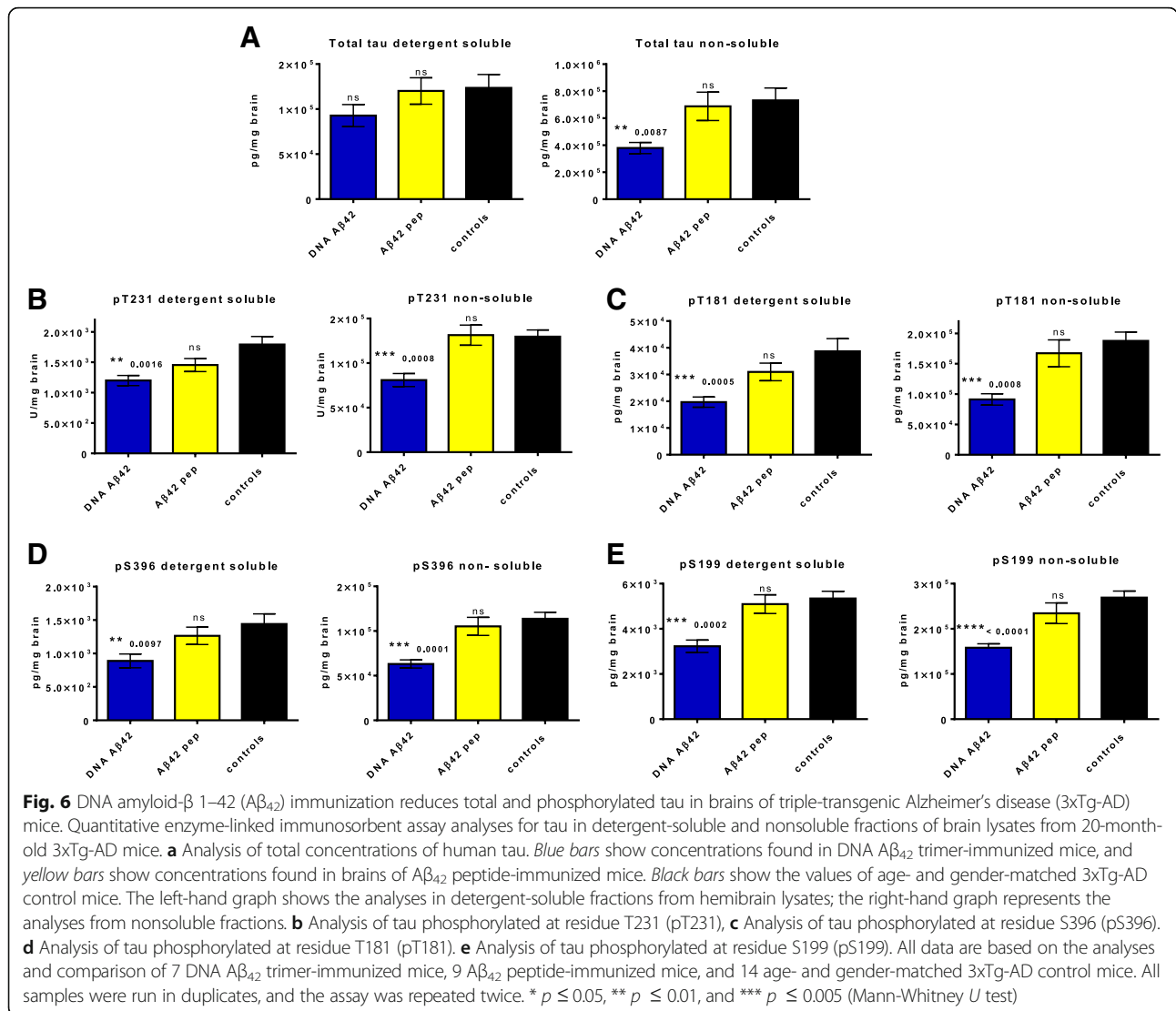
In comparison of the two A $\beta$  immunotherapies, a better reduction with high significance for phosphorylated tau molecules was found in DNA A $\beta$ 42 trimer-immunized mice. Percentages of reduction were calculated for the groups, and the results are shown in Table 1. A greater than 20% higher reduction was found in the detergent-soluble brain fractions of DNA-immunized mice for pT181 and pS396. This was statistically significant in the comparison of DNA- and peptide-immunized mice for pS396 ( $p < 0.0311$ ) (Table 1). For the nonsoluble brain fractions, 12–25% higher reductions were found in lysates from DNA A $\beta$ 42 trimer-immunized mice for total tau, pT231, pT181, and pS396. These values were statistically significant for the comparisons with the age- and gender-matched control mice (Fig. 6) and also in the comparison between the differently immunized groups of mice (Table 1).

#### Analyses of kinase variations

Western blot analyses were performed to detect whether different enzymatic kinase patterns could be found in brains from immunized mice. Significantly reduced levels of phosphorylated MEK (MAP2K), and phosphorylated ERK1/2 (p44/p42 mitogen-activated protein kinase [MAPK]), as well as reduced levels for the activated form of GSK3 $\beta$  (Y216), were found in brains from DNA-immunized mice. Figure 7 shows the detection MEK1/2 and phospho-MEK1/2 (Fig. 7a), as well as ERK1/2 and phosphorylated ERK1/2 (Fig. 7b), in brain lysates from seven DNA A $\beta$ 42-immunized mice compared with seven

age- and gender-matched 3xTg-AD control mice and two 20-month-old wild-type mice.

Results from the semiquantitative analysis of gray-level intensities (ImageJ software) are depicted in Fig. 8. Reductions in protein levels of phospho-MEK1/2 (Fig. 8a), total ERK1/2, and phospho-ERK1/2 (Fig. 8b) in DNA A $\beta$ 42-immunized mice were significant (*p* values of 0.0379, 0.0006, and 0.0087, respectively, by Mann-Whitney *U* test). Significant reductions were also found for protein levels of activated GSK3 $\beta$  ( $p = 0.0006$ ) (Fig. 8c). These data were further normalized against the protein levels of total MEK1/2, total ERK1/2, and total GSK $\alpha/\beta$  for each of the bands individually to compensate for the possibility of different overall protein levels for the tested enzymes in the brain lysates and shown as a percentage of protein (percentage of phosphorylated MEK, ERK, and GSK $\alpha/\beta$ ). The percentage difference for phospho-MEK1/2 was highly significant between control and DNA A $\beta$ 42-immunized mice ( $p = 0.0031$ ). In the comparison of phospho-ERK1/2 with total ERK1/2 in the DNA A $\beta$ 42-immunized mice, the reduction was not significant, because these mice already had less total ERK1/2. The percentage reduction of phospho-GSK3 $\beta$  (Y216) in the DNA A $\beta$ 42-immunized mice was highly significant ( $p = 0.006$ ). No differences in protein levels between the mouse groups were observed for the proteins MEK1/2 (Fig. 7a), GSK3 $\alpha/\beta$  (Fig. 7c), and the housekeeping protein  $\beta$ -tubulin (Fig. 7d). Of note, a blot with GSK3 $\alpha/\beta$  is shown in the comparison for activated GSK3 $\beta$  because it appears that there is weak cross-reactivity of this specific antibody with both GSK3 bands (Fig. 7c, lower panel), but differences were seen only for the strong reactivity with GSK3 $\beta$  phosphorylated at residue Y216 (46 kD band). Only this activated form of GSK3 $\beta$  is described and discussed. No significant differences were found for



total GSK3 $\beta$  protein levels in brain lysates from control and immunized mice (data not shown).

### Discussion

DNA  $A\beta_{42}$  immunotherapy results in significant reductions in  $A\beta_{42}$  peptide and plaque load in brains of the 3xTg-AD mouse model at 20 months of age, consistent with our previous results in double-transgenic mice [26, 27]. New findings shown with this vaccine for the first time were significant reductions of total tau and phosphorylated tau in brains of mice that had received active DNA  $A\beta_{42}$  trimer immunizations. This finding was confirmed by histology, Western blot analysis, and ELISA. Despite the 10 $\times$  levels of anti- $A\beta$  antibodies in peptide-immunized mice, peptide immunization was less efficacious, which is indicative of different  $A\beta$  species detected and removed by the antibodies generated

following DNA  $A\beta_{42}$  immunization (e.g.,  $A\beta$  oligomers). In fact, this was highly consistent throughout the study with more  $A\beta$  and more tau removed in DNA  $A\beta_{42}$  trimer-immunized mice than in  $A\beta_{42}$  peptide-immunized mice in all three assay systems used (immunohistology, Western blotting, ELISA). We had previously shown that the expression of the DNA  $A\beta_{42}$  trimer vaccine in skin shows production of  $A\beta$  oligomers [37]. We had also previously shown that the epitope specificity of antibodies produced after DNA  $A\beta_{42}$  immunization differs from the  $A\beta_{1-15}$  B-cell epitope specificity and shows a wide reactivity with epitopes across the  $A\beta_{1-42}$  peptide [38–40].  $A\beta$  oligomers in particular activate tau kinases, leading to hyperphosphorylation, and  $A\beta$  oligomers are also strong activators for cellular caspases, leading to tau cleavage and tau aggregation. Hyperphosphorylated tau and truncated tau are both prone to self-aggregation and tau accumulation in neurons, and phosphorylation of

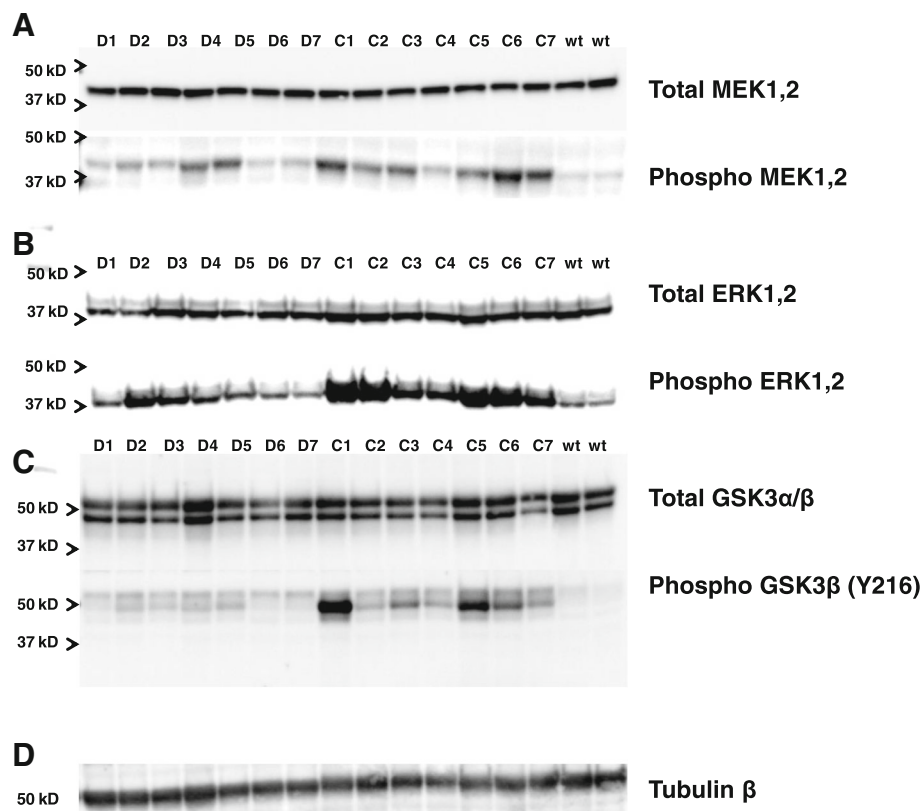


**Fig. 7** Significant changes in enzymes of the Ras/mitogen-activated protein kinase kinase (MEK)/extracellular signal-regulated kinase (ERK) signaling pathway and glycogen synthase kinase 3 $\beta$  (GSK3 $\beta$ ) following DNA amyloid- $\beta$  1–42 peptide ( $A\beta_{42}$ ) immunization. Equal amounts of proteins from soluble brain lysates of 20-month-old triple-transgenic Alzheimer's disease (3xTg-AD) mice (D1–D7 = DNA  $A\beta_{42}$ -immunized mice, C1–C7 = 3xTg-AD control mice, wt = wild-type control mice) were separated by SDS-PAGE, blotted onto nitrocellulose filters, and probed using antibodies specific for MEK (**a**, upper panel) and its active form phosphorylated MEK (**a** lower panel), total ERK1/2 (**b**, upper panel) and the phosphorylated forms of ERK1/2 (**b** lower panel), and GSK3 $\alpha/\beta$  (**c**, upper panel) and activated GSK3 $\beta$  (**c**, lower panel). Of note, a blot with GSK3 $\alpha/\beta$  is shown in the comparison for activated GSK3 $\beta$  because it appears that there was weak cross-reactivity of this specific antibody with both GSK3 bands (**c**, lower panel), but differences were seen only for the strong reactivity with GSK3 $\beta$  phosphorylated at residue Y216 (46 kD band). As a loading control, the blots were reprobed with the housekeeping protein  $\beta$ -tubulin (**d**). All assays were performed three times in independent experiments. Shown are representative results from one of these assays

specific residues in tau (e.g., S422) are important for caspase-mediated cleavage. Thus, less tau phosphorylation leads to less tau truncation via caspase-mediated cleavage and therefore reduces tau aggregation and total tau levels, explaining why  $A\beta_{42}$  immunization and reduction of  $A\beta_{42}$  peptides in brain led also to reduction of total tau [41–49].

DNA  $A\beta_{42}$  immunotherapy led to a noninflammatory immune response with no T-cell proliferation and no inflammatory cytokines produced during the cellular immune responses in the 3xTg-AD mouse model, similar to the immune responses we had found in the wild-type mouse model [22–25]. Although in the Balb/c wild-type mouse strain IgG1 was a dominant IgG antibody isotype in the humoral immune response [37], other mouse strains showed also a strong anti- $A\beta_{42}$  IgG2b antibody production similar to the one found in the 3xTg-AD mouse used in the present study (unpublished data).  $A\beta_{42}$  peptide immunization led to a mixed immune

response with high levels of all antibody isotypes, including IgG2a/c, and high levels of inflammatory cytokines in AD mouse models and wild-type mice [22–25, 28]. In a prime boost study, in which the immune response was first primed with  $A\beta_{42}$  peptide immunizations and then boosted with DNA  $A\beta_{42}$  immunizations in wild-type mice, we found that even though the anti- $A\beta_{42}$  antibody isotype profile had high levels of “inflammatory” IgG2a/c antibodies, no inflammatory cytokines were detected in the cellular in vitro assays, providing evidence that the DNA immunization resulted in the downregulation of inflammatory cellular responses [50]. Antibody isotypes strongly influence the therapeutic effect of a treatment or vaccine because the different antibody isotypes have different effector functions (complement binding, Fc receptor binding). In AD immunotherapy, microglial activation is thought to help remove excess  $A\beta$  from the brain, so that FcR binding is not a negative feature of the antibody per se. Furthermore, the epitope detected

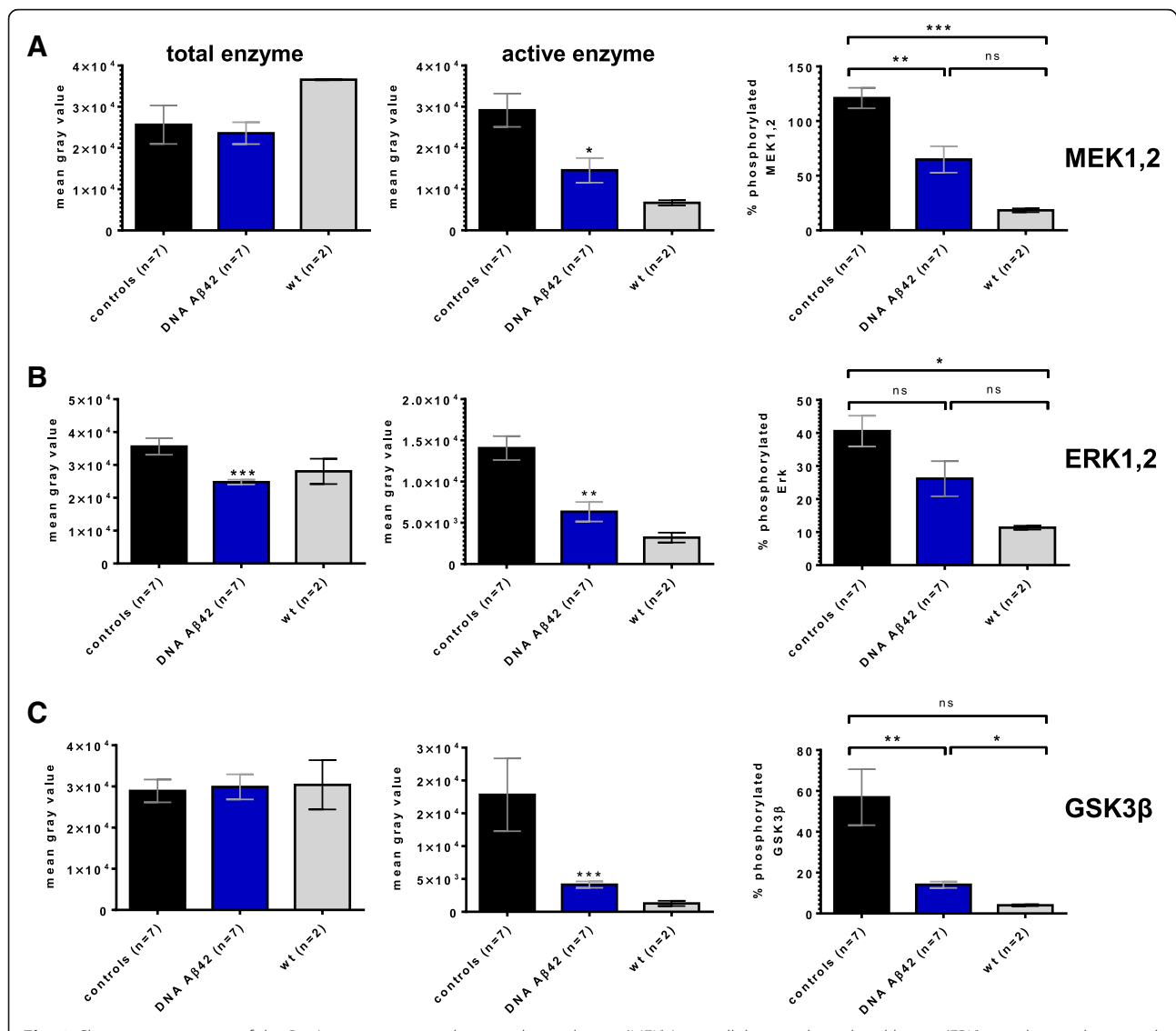


**Fig. 8** Changes in enzymes of the Ras/mitogen-activated protein kinase kinase (MEK)/extracellular signal-regulated kinase (ERK) signaling pathway and glycogen synthase kinase 3β (GSK3β) following DNA amyloid-β 1–42 peptide (Aβ<sub>42</sub>) immunization. Gray-level intensities (arbitrary units) of the protein bands from the Western blots shown in Fig. 7 were semiquantitatively analyzed using the ImageJ software package (National Institutes of Health). *Black bars* represent levels found in triple-transgenic Alzheimer's disease (3xTg-AD) control mice ( $n = 7$ ); *blue bars* represent levels found in DNA Aβ<sub>42</sub> trimer-immunized mice ( $n = 7$ ); and *gray bars* represent levels in wild-type mice ( $n = 2$ ). **a** Analyses for MEK. **b** Analyses for ERK. **c** Analyses for GSK3β. The first graph in each row shows gray-level intensities for total enzyme; the second graph shows gray-level intensities for the active (phosphorylated) forms of the respective kinases; and the third graph shows the normalized data in which the levels of the phosphorylated kinases were calculated as a percentage of the total enzyme levels for each of the mouse brain lysates used. \*, \*\*, and \*\*\* indicate  $p$  values of  $\leq 0.05$ ,  $\leq 0.01$  and  $\leq 0.005$ , respectively (Mann-Whitney  $U$  test)

by the respective antibody pool is crucial for removal of amyloid from the brain [51–53]. Thus, the multivalent nature of the humoral immune response following DNA Aβ<sub>42</sub> immunization is beneficial in many aspects.

To address how either DNA Aβ<sub>42</sub> or Aβ peptide vaccinations can cause both Aβ and tau reduction, we investigated a number of kinases involved in tau phosphorylation that had also been shown to be activated by Aβ<sub>42</sub> peptides and in particular Aβ<sub>42</sub> oligomers [54–56]. We were able to show differences for the activated/phosphorylated kinases MEK1/2, p40/p42 MAPK1

and MAPK2 (ERK1/2), and GSK-3β in brain protein lysates from female DNA Aβ<sub>42</sub>-immunized mice compared with the age- and gender (female)-matched 3xTg-AD control mice, supportive of the assumption that a higher removal of Aβ oligomers after DNA Aβ<sub>42</sub> trimer immunization has significant effects on tau pathology via changes on cellular kinases. ERK1 and ERK2 are both highly expressed in the brain, and it had been shown in vitro that ERK2 is capable of phosphorylating a large number of residues in tau. Activation of the RAS-RAF-MEK-ERK signaling pathway by APP and

A $\beta_{42}$  oligomers in a cell culture system as well as in postmortem human AD brains indicated a pathologic link between A $\beta$  and this particular MAPK pathway [57–59]. It has been suggested by others that the two main pathologies of AD, amyloid and tau aggregation, affect the aging brain and cause changes in large-scale neuronal circuits [60]. We show in the present study that DNA A $\beta_{42}$  immunization led to significant changes in several pathways. Further analyses of the mechanism of action on tau reduction and changes in cellular signaling pathways in the DNA A $\beta_{42}$  trimer-immunized mice are goals for future research.

It had been shown before in the 3xTg-AD mouse model that antitau immunotherapy or passive anti-A $\beta$  immunotherapy led to removal of tau or A $\beta$  or both [19, 43, 55, 61–64]. Of note, these studies were of passive immunotherapy using preformed mAbs or the intracranial injection of anti-A $\beta$  or antitau antibodies, which is different from the active immunization done in the present study. It had also been shown before that immunization with a DNA vaccine encoding A $\beta_{1-11}$  or a short tau epitope led to the production of antibodies against A $\beta$  or tau, respectively [65, 66]. We show for the first time a different mechanism in which active DNA A $\beta_{42}$  trimer immunization in the 3xTg-AD mouse model results in reduction of both pathologies with one vaccine: A $\beta$  reduction due to antibodies generated against A $\beta$  and tau reduction due to an indirect mechanism in which less A $\beta$  led to less tau kinase activation and therefore to less tau phosphorylation. Of note, also in AN-1792, a clinical trial using A $\beta_{42}$  immunotherapy in patients with AD, a trend toward reduction in cerebrospinal fluid phospho-tau concentrations was reported, and analysis of postmortem brain tissue showed a reduction of aggregated tau in neuronal processes [1–3, 67].

Current assessments of A $\beta$  immunotherapy for the prevention of AD in several completed and ongoing trials show divergent responses [68]. Positive results in patients treated with the mAb aducanumab support the effectiveness of A $\beta$  immunotherapy in patients with early AD [8]. Aducanumab is a fully human IgG1 antibody that corresponds to the IgG2a antibody isotype in the mouse. Of note, aducanumab has been characterized as an antibody that binds to soluble A $\beta_{42}$  oligomers and insoluble A $\beta_{42}$  fibrils prepared in vitro, but not A $\beta_{42}$  monomers, consistent with the detection of conformational but not linear epitopes. This antibody reactivity might be similar to antibodies generated in response to immunization with DNA A $\beta_{42}$  trimer as shown in the present study.

## Conclusions

We present data showing for the first time that active immunization with a DNA plasmid coding for an A $\beta$  trimer (3xA $\beta_{1-42}$ ) designed to induce an anti-A $\beta$  humoral

immune response in the 3xTg-AD mouse model significantly reduced both of the main AD pathologies, amyloid and tau. We show a significant reduction in activated protein levels for p44/p44 MAPK (ERK1/2), the upstream MEK, and GSK3 $\beta$ . Our data support significant changes in the Ras-Raf-MEK-ERK signaling pathway in AD mouse model brain due to DNA A $\beta_{42}$  immunotherapy, and this is a goal of further studies. DNA A $\beta_{42}$  immunization in patients with AD has the potential to modify early and late changes in this disease. It is expected that DNA A $\beta_{42}$  trimer immunotherapy in a clinical trial will reduce both plaques and tangles in patients with AD.

## Abbreviations

AD: Alzheimer's disease; ANOVA: Analysis of variance; APP: Amyloid precursor protein; A $\beta_{42}$ : Amyloid- $\beta$  peptide 1–42; DTT: Dithiothreitol; EGTA: Ethylene glycol-bis( $\beta$ -aminoethyl ether)-*N,N,N',N'*-tetraacetic acid; ELISA: Enzyme-linked immunosorbent assay; ELISPOT: Enzyme-linked immunospot; ERK: Extracellular signal-regulated kinase; GAPDH: Glyceraldehyde 3-phosphate dehydrogenase; GSK3 $\beta$ : Glycogen synthase kinase 3 $\beta$ ; IFN: Interferon; Ig: Immunoglobulin; IL: Interleukin; mAb: Monoclonal antibody; MAPK: Mitogen-activated protein kinase; MEK: Mitogen-activated protein kinase kinase; PFA: Paraformaldehyde

## Acknowledgements

We thank the UTSW Whole Brain Microscopy Facility (WBMF) in the Department of Neurology and Neurotherapeutics for assistance with slide scanning. WBMF is supported by the Texas Institute for Brain Injury and Repair (TIBIR).

## Funding

The research reported in this publication was supported by National Institute on Aging/National Institutes of Health (NIH) grant P30AG12300-21; the Zale Foundation; the Rudman Foundation; Presbyterian Village North Foundation; Freiburger, Losinger, and Denker Family Funds; "Triumph over Alzheimer's" Charity; AWARE; the National Center for Advancing Translational Sciences of the NIH under Center for Translational Medicine award number UL1TR001105; and a grant from the Friends of the Alzheimer's Disease Center.

## Availability of data and materials

Not applicable.

## Authors' contributions

RNR planned the experiments, discussed the results, and wrote and revised the paper. MF planned and did the experiments and helped with the editing of the manuscript. DLW planned and performed the experiments, analyzed and discussed the data, and wrote and revised the paper. All authors read and approved the final manuscript.

## Ethics approval

Animal use for this study was approved by the Institutional Animal Care and Use Committee at UTSW.

## Consent for publication

Not applicable.

## Competing interests

The authors declare that they have no competing interests.

## Publisher's Note

Springer Nature remains neutral with regard to jurisdictional claims in published maps and institutional affiliations.

Received: 15 March 2018 Accepted: 12 October 2018

Published online: 20 November 2018

## References

- Orgogozo JM, Gilman S, Dartigues JF, Laurent B, Puel M, Kirby LC, Jouanny P, Dubois B, Eisner L, Flitman S, Michel BF, Boada M, Frank A, Hock C. Subacute meningoencephalitis in a subset of patients with AD after A $\beta$ <sub>42</sub> immunization. *Neurology*. 2003;61(1):46–54.
- Fox NC, Black RS, Gilman S, Rossor MN, Griffith SG, Jenkins L, Koller M, AN1792(QS-21)-201 Study. Effects of A $\beta$  immunization (AN1792) on MRI measures of cerebral volume in Alzheimer disease. *Neurology*. 2005;64:1563–72.
- Gilman S, Koller M, Black RS, Jenkins L, Griffith SG, Fox NC, Eisner L, Kirby L, Rovira MB, Forette F, Orgogozo JM, AN1792(QS-21)-201 Study Team. Clinical effects of A $\beta$  immunization (AN1792) in patients with AD in an interrupted trial. *Neurology*. 2006;64:1553–62.
- Blennow K, Zetterberg H, Rinne JO, Salloway S, Wei J, Black R, Grundman M, Liu E, AAB-001 201/202 Investigators. Effect of immunotherapy with bapineuzumab on cerebrospinal fluid biomarker levels in patients with mild to moderate Alzheimer disease. *Arch Neurol*. 2011;69(8):1002–10.
- Adolfsson O, Pihlgren M, Toni N, Varisco Y, Buccarello AL, Antonielli K, Lohmann S, Piorkowska K, Gafner V, Atwal JK, Maloney J, Chen M, Gogineni A, Weimer RM, Mortensen DL, Friesenhahn M, Ho C, Paul R, Pfeifer A, Muhs A, Watts RJ. An effector-reduced anti- $\beta$ -amyloid (A $\beta$ ) antibody with unique A $\beta$  binding properties promotes neuroprotection and glial engulfment of A $\beta$ . *J Neurosci*. 2012;32(28):9677–89.
- Bohrmann B, Baumann K, Benz J, Gerber F, Huber W, Knoflach F, Messer J, Oroszlan K, Rauchenberger R, Richter WF, Rothe C, Urban M, Bardroff M, Winter M, Nordstedt C, Loetscher H. Gantenerumab: a novel human anti-A $\beta$  antibody demonstrates sustained cerebral amyloid- $\beta$  binding and elicits cell-mediated removal of human amyloid- $\beta$ . *J Alzheimers Dis*. 2012;28(1):49–69.
- Farlow M, Arnold SE, van Dyck CH, Aisen PS, Snider BJ, Porsteinsson AP, Friedrich S, Dean RA, Gonzales C, Sethuraman G, DeMattos RB, Mohs R, Paul SM, Siemers ER. Safety and biomarker effects of solanezumab in patients with Alzheimer's disease. *Alzheimers Dement*. 2012;8(4):261–71.
- Sevigny J, Chiao P, Bussièrè T, Weinreb PH, Williams L, Maier M, Dunstan R, Salloway S, Chen T, Ling Y, O'Gorman J, Qian F, Arastu M, Li M, Chollate S, Brennan MS, Quintero-Monzon O, Scannevin RH, Arnold HM, Engber T, Rhodes K, Ferrero J, Hang Y, Mikulskis A, Grimm J, Hock C, Nitsch RM, Sandrock A. The antibody aducanumab reduces A $\beta$  plaques in Alzheimer's disease. *Nature*. 2016;537(7618):50–6.
- Iqbal K, Liu F, Gong CX. Tau and neurodegenerative disease: the story so far. *Nat Rev Neurol*. 2016;1:15–27.
- Novak P, Schmidt R, Kontsejkova E, Zilka N, Kovacech B, Skrabana R, Vince-Kazmerova Z, Katina S, Fialova L, Prcina M, Parrak V, Dal-Bianco P, Brunner M, Staffen W, Rainer M, Ondrus M, Ropole S, Smisek M, Sivak R, Winblad B, Novak M. Safety and immunogenicity of the tau vaccine AADvac1 in patients with Alzheimer's disease: a randomised, double-blind, placebo-controlled, phase 1 trial. *Lancet Neurol*. 2017;16(2):123–34.
- Kontsejkova E, Zilka N, Kovacech B, Novak P, Novak M. First-in-man tau vaccine targeting structural determinants essential for pathological tau-tau interaction reduces tau oligomerisation and neurofibrillary degeneration in an Alzheimer's disease model. *Alzheimers Res Ther*. 2014;6:44.
- Levites Y, Sinyavskaya O, Rosario AM, Cruz PE, Lewis J, Golde TE. Targeting intra vs extracellular tau by recombinant antibodies [abstract]. *Neurodegener Dis*. 2015;15(Suppl 1):337.
- Sigurdsson EM. Tau immunotherapy. *Neurodegener Dis*. 2016;16(1–2):34–8.
- Theunis C, Crespo-Biel N, Gafner V, Pihlgren M, López-Deber MP, Reis P, Hickman DT, Adolfsson O, Chuard N, Ndao DM, Borghgraef P, Devijver H, van Leuven F, Pfeifer A, Muhs A. Efficacy and safety of a liposome-based vaccine against protein Tau, assessed in tau.P301L mice that model tauopathy. *PLoS One*. 2013;8:e72301.
- Troquier L, Caillierez M, Burnouf S, Fernandez-Gomez FJ, Grosjean MJ, Zommer N, Sergeant N, Schraen-Maschke S, Blum D, Buee L. Targeting phospho-Ser422 by active Tau immunotherapy in the THY-Tau22 mouse model: a suitable therapeutic approach. *Curr Alzheimer Res*. 2012;9:397–405.
- Congdon EE, Gu J, Sait HB, Sigurdsson EM. Antibody uptake into neurons occurs primarily via clathrin-dependent Fc $\gamma$  receptor endocytosis and is a prerequisite for acute tau protein clearance. *J Biol Chem*. 2013;288:35452–65.
- Gu J, Congdon EE, Sigurdsson EM. Two novel Tau antibodies targeting the 396/404 region are primarily taken up by neurons and reduce Tau protein pathology. *J Biol Chem*. 2013;288:33081–95.
- Iltner A, Bertz J, Suh LS, Stevens CH, Götz J, Iltner LM. Tau-targeting passive immunization modulates aspects of pathology in tau transgenic mice. *J Neurochem*. 2015;132:135–45.
- Walls KC, Ager RR, Vasilevko V, Cheng D, Medeiros R, LaFerla FM. p-Tau immunotherapy reduces soluble and insoluble tau in aged 3xTg-AD mice. *Neurosci Lett*. 2014;575:96–100.
- Yanamandra K, Kfoury N, Jiang H, Mahan TE, Ma S, Maloney SE, Wozniak DF, Diamond MI, Holtzman DM. Anti-tau antibodies that block tau aggregate seeding in vitro markedly decrease pathology and improve cognition in vivo. *Neuron*. 2013;80:402–14.
- Kutzler MA, Weiner DB. DNA vaccines: ready for prime time? *Nat Rev Genet*. 2008;9(10):776–88.
- Lambracht-Washington D, Qu BX, Fu M, Eagar TN, Stüve O, Rosenberg RN. DNA  $\beta$ -amyloid (1–42) trimer immunization for Alzheimer disease in a wild-type mouse model. *JAMA*. 2009;302(16):1796–802.
- Lambracht-Washington D, Qu BX, Fu M, Eagar TN, Stüve O, Rosenberg RN. DNA immunization against amyloid  $\beta$  42 has high potential as safe therapy for Alzheimer's disease as it diminishes antigen specific Th1 and Th17 cell proliferation. *Cell Mol Neurobiol*. 2011;31:867–74.
- Lambracht-Washington D, Rosenberg RN. Co-stimulation with TNF receptor superfamily 4/25 antibodies enhances in-vivo expansion of CD4<sup>+</sup>CD25<sup>+</sup>Foxp3<sup>+</sup> T cells (Tregs) in a mouse study for active DNA A $\beta$ <sub>42</sub> immunotherapy. *J Neuroimmunol*. 2015;278:90–9.
- Lambracht-Washington D, Rosenberg RN. A non-inflammatory immune response in aged DNA A $\beta$ <sub>42</sub> immunized mice supports its safety for possible use as immunotherapy in AD patients. *Neurobiol Aging*. 2015;36(3):1274–81.
- Qu B-X, Xiang Q, Li L, Johnston SA, Hynan LS, Rosenberg RN. A $\beta$ <sub>42</sub> gene vaccine prevents A $\beta$ <sub>42</sub> deposition in brain of double transgenic mice. *J Neurol Sci*. 2007;260:204–13.
- Lambracht-Washington D, Rosenberg RN. Active DNA A $\beta$ <sub>42</sub> vaccination as immunotherapy for Alzheimer disease. *Transl Neurosci*. 2012;3(4):307–13.
- Rosenberg RN, Lambracht-Washington D, Yu G, Xia W. Genomics of Alzheimer disease: a review. *JAMA Neurol*. 2016;73(7):867–74.
- Oddo S, Caccamo A, Shepherd JD, Murphy MP, Golde TE, Kaye R, Metherate R, Mattson MP, Akbari Y, LaFerla FM. Triple-transgenic model of Alzheimer's disease with plaques and tangles: intracellular A $\beta$  and synaptic dysfunction. *Neuron*. 2003;39(3):409–21.
- Oddo S, Caccamo A, Kitazawa M, Tseng BP, LaFerla FM. Amyloid deposition precedes tangle formation in a triple transgenic model of Alzheimer's disease. *Neurobiol Aging*. 2003;24(8):1063–70.
- Kilkenny C, Browne WJ, Cuthill IC, Emerson M, Altman DG. Improving bioscience research reporting: the ARRIVE guidelines for reporting animal research. *PLoS Biol*. 2010;8(6):e1000412.
- Schneider CA, Rasband WS, Eliceiri KW. NIH Image to ImageJ: 25 years of image analysis. *Nat Methods*. 2012;9(7):671–5.
- Grant SM, Ducatenzeiler A, Szyf M, Cuello AC. A $\beta$  immunoreactive material is present in several intracellular compartments in transfected, neuronally differentiated, P19 cells expressing the human amyloid  $\beta$ -protein precursor. *J Alzheimers Dis*. 2000;2(3–4):207–22.
- Iulita MF, Allard S, Richter L, Munter LM, Ducatenzeiler A, Weise C, Do Carmo S, Klein WL, Multhaup G, Cuello AC. Intracellular A $\beta$  pathology and early cognitive impairments in a transgenic rat overexpressing human amyloid precursor protein: a multidimensional study. *Acta Neuropathol Commun*. 2014;2:61.
- Augustinack JC, Schneider A, Mandelkow EM, Hyman BT. Specific tau phosphorylation sites correlate with severity of neuronal cytopathology in Alzheimer's disease. *Acta Neuropathol*. 2002;103(1):26–35.
- Sahara N, DeTure M, Ren Y, Ebrahim AS, Kang D, Knight J, Volbracht C, Pedersen JT, Dickson DW, Yen SH, Lewis J. Characteristics of TBS-extractable hyperphosphorylated tau species: aggregation intermediates in rTg4510 mouse brain. *J Alzheimers Dis*. 2013;33(1):249–63.
- Qu BX, Lambracht-Washington D, Fu M, Eagar TN, Stüve O, Rosenberg RN. Analysis of three plasmid systems for use in DNA A $\beta$ <sub>42</sub> immunization as therapy for Alzheimer's disease. *Vaccine*. 2010;28:5280–7.
- Lambracht-Washington D, Rosenberg RN. DNA A $\beta$ <sub>42</sub> immunization generates a multivalent vaccine: antibodies in plasma of active full-length DNA A $\beta$ <sub>42</sub> immunized mice show polyclonal A $\beta$ <sub>42</sub> peptide binding [abstract]. *Alzheimers Dement*. 2015;11(7 Suppl):P842.

39. Lambracht-Washington D, Fu M, Wight-Carter M, Riegel M, Rosenberg RN. Evaluation of a DNA A $\beta_{42}$  vaccine in aged NZW rabbits: antibody kinetics and immune profile after intradermal immunization with full-length DNA A $\beta_{42}$  trimer. *J Alzheimers Dis*. 2017;57(1):97–112.
40. Lambracht-Washington D, Fu M, Frost P, Rosenberg RN. Evaluation of a DNA A $\beta_{42}$  vaccine in adult rhesus monkeys (*Macaca mulatta*): antibody kinetics and immune profile after intradermal immunization with full-length DNA A $\beta_{42}$  trimer. *Alzheimers Res Ther*. 2017;9(1):30.
41. Chong YH, Shin YJ, Lee EO, Kayed R, Glabe CG, Tenner AJ. ERK1/2 activation mediates A $\beta$  oligomer-induced neurotoxicity via caspase-3 activation and tau cleavage in rat organotypic hippocampal slice cultures. *J Biol Chem*. 2006;281(29):20315–25.
42. Guillozet-Bongaarts AL, Cahill ME, Cryns VL, Reynolds MR, Berry RW, Binder LI. Pseudophosphorylation of tau at serine 422 inhibits caspase cleavage: in vitro evidence and implications for tangle formation in vivo. *J Neurochem*. 2006;97(4):1005–14.
43. Oddo S, Billings L, Kesslak JP, Cribbs DH, LaFerla FM. A $\beta$  immunotherapy leads to clearance of early, but not late, hyperphosphorylated tau aggregates via the proteasome. *Neuron*. 2004;43(3):321–32.
44. Oddo S, Caccamo A, Tran L, Lambert MP, Glabe CG, Klein WL, LaFerla FM. Temporal profile of amyloid- $\beta$  (A $\beta$ ) oligomerization in an in vivo model of Alzheimer disease: a link between A $\beta$  and tau pathology. *J Biol Chem*. 2006;281(3):1599–604.
45. Rissman RA, Poon WW, Blurton-Jones M, Oddo S, Torp R, Vitek MP, LaFerla FM, Rohn TT, Cotman CW. Caspase-cleavage of tau is an early event in Alzheimer disease tangle pathology. *J Clin Invest*. 2004;114(1):121–30.
46. Cho JH, Johnson GV. Glycogen synthase kinase 3 $\beta$  induces caspase-cleaved tau aggregation in situ. *J Biol Chem*. 2004;279(52):54716–23.
47. Gamblin TC, Chen F, Zambrano A, Abraha A, Lagalwar S, Guillozet AL, Lu M, Fu Y, Garcia-Sierra F, LaPointe N, Miller R, Berry RW, Binder LI, Cryns VL. Caspase cleavage of tau: linking amyloid and neurofibrillary tangles in Alzheimer's disease. *Proc Natl Acad Sci U S A*. 2003;100(17):10032–7.
48. Delobel P, Lavenir I, Fraser G, Ingram E, Holzer M, Ghetti B, Spillantini MG, Crowther RA, Goedert M. Analysis of tau phosphorylation and truncation in a mouse model of human tauopathy. *Am J Pathol*. 2008;172(1):123–31.
49. Mead E, Kestoras D, Gibson Y, Hamilton L, Goodson R, Jones S, Eversden S, Davies P, O'Neill M, Hutton M, Szekeles P, Wolak J. Halting of caspase activity protects tau from MCI-conformational change and aggregation. *J Alzheimers Dis*. 2016;54(4):1521–38.
50. Lambracht-Washington D, Qu BX, Fu M, Anderson LD Jr, Eagar TN, Stüve O, Rosenberg RN. A peptide prime-DNA boost immunization protocol provides significant benefits as a new generation A $\beta_{42}$  DNA vaccine for Alzheimer disease. *J Neuroimmunol*. 2013;254(1–2):63–8.
51. Nimmerjahn F, Ravetch JV. Divergent immunoglobulin G subclass activity through selective Fc receptor binding. *Science*. 2005;310(5753):1510–2.
52. Huber VC, McKeon RM, Brackin MN, Miller LA, Keating R, Brown SA, Makarova N, Perez DR, Macdonald GH, McCullers JA. Distinct contributions of vaccine-induced immunoglobulin G1 (IgG1) and IgG2a antibodies to protective immunity against influenza. *Clin Vaccine Immunol*. 2006;13(9):981–90.
53. Beers SA, Glennie MJ, White AL. Influence of immunoglobulin isotype on therapeutic antibody function. *Blood*. 2016;127(9):1097–101.
54. Zago W, Buttini M, Comery TA, Nishioka C, Gardai SJ, Seubert P, Games D, Bard F, Schenk D, Kinney GG. Neutralization of soluble, synaptotoxic amyloid  $\beta$  species by antibodies is epitope specific. *J Neurosci*. 2012;32(8):2696–702.
55. Rasool S, Martinez-Coria H, Wu JW, LaFerla F, Glabe CG. Systemic vaccination with anti-oligomeric monoclonal antibodies improves cognitive function by reducing A $\beta$  deposition and tau pathology in 3xTg-AD mice. *J Neurochem*. 2013;126(4):473–82.
56. Kirouac L, Rajic AJ, Cribbs DH, Padmanabhan J. Activation of Ras-ERK signaling and GSK-3 by amyloid precursor protein and amyloid B Facilitates neurodegeneration in Alzheimer's disease. *eNeuro*. 2017;4(2):e0149–16.201.
57. Kim EK, Choi EJ. Pathological roles of MAPK signaling pathways in human diseases. *Biochim Biophys Acta*. 2010;1802(4):396–405.
58. Ferrer I, Blanco R, Carmona M, Puig B. Phosphorylated mitogen-activated protein kinase (MAPK/ERK-P), protein kinase of 38 kDa (p38-P), stress-activated protein kinase (SAPK/JNK-P), and calcium/calmodulin-dependent kinase II (CaM kinase II) are differentially expressed in tau deposits in neurons and glial cells in tauopathies. *J Neural Transm (Vienna)*. 2001;108(12):1397–415.
59. Qi H, Prabakaran S, Cantrelle FX, Chambraud B, Gunawardena J, Lippens G, Landrieu I. Characterization of neuronal tau protein as a target of extracellular signal-regulated kinase. *J Biol Chem*. 2016;291(14):7742–53.
60. Sepulcre J, Sabuncu MR, Li Q, El Fakhri G, Sperling R, Johnson KA. Tau and amyloid- $\beta$  proteins distinctively associate to functional network changes in the aging brain. *Alzheimers Dement*. 2017;13(11):1261–9.
61. Dai CL, Tung YC, Liu F, Gong CX, Iqbal K. Tau passive immunization inhibits not only tau but also A $\beta$  pathology. *Alzheimers Res Ther*. 2017;9(1):1.
62. Oddo S, Vasilevko V, Caccamo A, Kitazawa M, Cribbs DH, LaFerla FM. Reduction of soluble A $\beta$  and tau, but not soluble A $\beta$  alone, ameliorates cognitive decline in transgenic mice with plaques and tangles. *J Biol Chem*. 2006;281(51):39413–23.
63. Lathuilière A, Laverenne V, Astolfo A, Kopetzki E, Jacobsen H, Stampanoni M, Bohrmann B, Schneider BL, Aebischer P. A subcutaneous cellular implant for passive immunization against amyloid- $\beta$  reduces brain amyloid and tau pathologies. *Brain*. 2016;139(Pt 5):1587–604.
64. Castillo-Carranza DL, Guerrero-Muñoz MJ, Sengupta U, et al. Tau immunotherapy modulates both pathological tau and upstream amyloid pathology in an Alzheimer's disease mouse model. *J Neurosci*. 2015;35(12):4857–68.
65. Movsesyan N, Ghochikyan A, Mkrtichyan M, Petrushina I, Davtyan H, Olkhanud PB, Head E, Biragyn A, Cribbs DH, Agadjanyan MG. Reducing AD-like pathology in 3xTg-AD mouse model by DNA epitope vaccine - a novel immunotherapeutic strategy. *PLoS One*. 2008;3(5):e2124.
66. Davtyan H, Zagorski K, Rajapaksha H, Hovakimyan A, Davtyan A, Petrushina I, Kazarian K, Cribbs DH, Petrovsky N, Agadjanyan MG, Ghochikyan A. Alzheimer's disease Advax(CpG)-adjuvanted MultiTEP-based dual and single vaccines induce high-titer antibodies against various forms of tau and A $\beta$  pathological molecules. *Sci Rep*. 2016;6:28912.
67. Boche D, Donald J, Love S, et al. Reduction of aggregated Tau in neuronal processes but not in the cell bodies after A $\beta_{42}$  immunization in Alzheimer's disease. *Acta Neuropathol*. 2010;120(1):13–20.
68. Abbott A, Dolgin E. News in focus: leading Alzheimer's theory survives drug failure. *Nature*. 2016;540:15–6.

**Ready to submit your research? Choose BMC and benefit from:**

- fast, convenient online submission
- thorough peer review by experienced researchers in your field
- rapid publication on acceptance
- support for research data, including large and complex data types
- gold Open Access which fosters wider collaboration and increased citations
- maximum visibility for your research: over 100M website views per year

**At BMC, research is always in progress.**

Learn more [biomedcentral.com/submissions](https://www.biomedcentral.com/submissions)

